

# Three-dimensional printing of alginate: From seaweeds to heart valve scaffolds

Albert Ryszard Liberski\*

Sidra Medical and Research Center,  
P.O. Box 26999, Doha, Qatar  
\*Email: aliberski@sidra.org

## ABSTRACT

Three-dimensional (3D) printing is a resourceful technology that offers a large selection of solutions that are readily adaptable to tissue engineering of artificial heart valves (HVs). Different deposition techniques could be used to produce complex architectures, such as the three-layered architecture of leaflets. Once the assembly is complete, the growth of cells in the scaffold would enable the deposition of cell-specific extracellular matrix proteins. 3D printing technology is a rapidly evolving field that first needs to be understood and then explored by tissue engineers, so that it could be used to create efficient scaffolds. On the other hand, to print the HV scaffold, a basic understanding of the fundamental structural and mechanical aspects of the HV should be gained. This review is focused on alginate that can be used as a building material due to its unique properties confirmed by the successful application of alginate-based biomaterials for the treatment of myocardial infarction in humans. Within the field of biomedicine, there is a broad scope for the application of alginate including wound healing, cell transplantation, delivery of bioactive agents, such as chemical drugs and proteins, heat burns, acid reflux, and weight control applications. The non-thrombogenic nature of this polymer has made it an attractive candidate for cardiac applications, including scaffold fabrication for heart valve tissue engineering (HVTE). The next essential property of alginate is its ability to form films, fibers, beads, and virtually any shape in a variety of sizes. Moreover, alginate possesses several prime properties that make it suitable for use in free-form fabrication techniques. The first property is its ability, when dissolved, to increase the viscosity of aqueous solutions, which is particularly important in formulating extrudable mixtures for 3D printing. The second property is its ability to form gels in mild conditions, for example, by adding calcium salt to an aqueous solution of alginate. The latter property is a basis for reactive extrusion- and inkjet printing-based solid free-form fabrication. Both techniques enable the production of scaffolds for cell encapsulation, which increases the seeding efficiency of fabricated structures. The objective of this article is to review methods for the fabrication of alginate hydrogels in the context of HVTE.

*Keywords:* Three-dimensional printing, Heart Valve, Tissue Engineering, Alginate, Hydrogels, living threads

[http://dx.doi.org/  
10.5339/connect.2016.3](http://dx.doi.org/10.5339/connect.2016.3)

Submitted: 11 November 2015  
Accepted: 29 February 2016  
© 2016 Liberski, licensee HBKU  
Press. This is an open access article  
distributed under the terms of the  
Creative Commons Attribution  
license CC BY 4.0, which permits  
unrestricted use, distribution and  
reproduction in any medium,  
provided the original work is  
properly cited.

## 1. INTRODUCTION

“Blue sky” tissue engineering is an extravagance that cannot be afforded today. Tissue engineering needs to overcome specific problems and limitations to currently used solutions that are encountered by clinicians. This demand necessitates continued communication and information flow between tissue engineers and clinicians. It is remarkable to see how much discrepancy is still present between current possibilities and medics’ expectation in relation to free-form fabrication techniques. Having a desktop device standing in the corner of the operating theater, providing ready-to-use patient-customized functional organs on demand, is perhaps realistic, but still a distant vision. To be efficient, we need to be realistic and practical. To help with this, we discussed current achievements in 3D biopolymer deposition for tissue engineering, and to navigate efficiently, we chose to narrow the field to alginate hydrogel fabrication methods presented in the context of heart valve tissue engineering (HVTE).

This paper is organized as follows. Section 2 discusses the properties of alginate and its current biomedical applications. Section 3 gives a brief overview of current challenges related to the development of the artificial heart valve (HV) that will mimic the functions of a native valve. Section 4 describes the types and basic features of 3D printers associated with the shaping of alginates, and shows how the role of the printer operator depends on the type of printer. Sections 5 and 6 discuss the principal methods for free-form fabrication of alginate-based structures, namely inkjet printing- and extrusion-based deposition, respectively. These sections aim to show the limitations and advantages of both strategies. As there are only a limited number of groups focused on HVTE, we report other cases to show how a given procedure can be adapted to HVTE. We believe that this would be a standard exercise for those tissue engineers who are trying to implement three-dimensional (3D) deposition as a tool in their workflow.

Section 7 discusses current work on 3D printing of the HV, and highlights the gap between the current state-of-the-art and a structurally adequate, functional construct capable of replacing the HV. This section addresses the topic of instrumentation cost, and shows how groundbreaking research may be conducted using in-house customized, low-cost equipment. This would help prevent adepts of free-form fabrication from overpaying for instruments that are not adjusted to their needs or level of expertise. Section 8 reveals that patterning of extruded threads is in principle similar to other yarn processing techniques such as weaving. Weaving is a very mature technology compared with 3D printing; textile techniques should also be considered as a powerful free-form fabrication tool. Furthermore, Section 9 clearly identifies the present research direction as obtaining an alginate-based HV scaffold structure. In this way, we intend to fend off allegations of being subjective in selecting examples from the reviewed literature. Section 10 describes “new kids on the block” in the field of alginate fabrication. With the first few examples of the literature available, we settle our conviction that they are an early manifestation of the new direction of further development. Finally, Section 11 explains why this review cannot and would not be complete; the revolution of 3D fabrication is advancing rapidly. Thus, our only ambition is to leave the landmark that summarizes the current state-of-the-art. In a year or two, this landmark will be far behind the advancing front lines. Nevertheless, we believe that adepts will benefit from reading this paper and pioneers will get well-deserved credit for their early involvement.

## 2. GENERAL PROPERTIES OF ALGINATE

Alginate is a naturally occurring polysaccharide mainly extracted from brown seaweeds, and has been widely used as a hydrogel for tissue engineering.<sup>1</sup> Alginates can be prepared with a wide range of molecular weights (e.g., 32–400 kDa)<sup>1–3</sup> and are characterized by long chains that contain two different acidic components, namely  $\alpha$ -L-guluronic acid (G) and 1,4-linked  $\beta$ -D-mannuronic acid (M).

The overall M/G ratio and the way in which the G and M units are arranged in the chain can vary from one species of seaweed to another. The origin and conditions of the extraction procedure can affect the viscosity of aqueous alginate solutions, lowering it if conditions are too arduous.

The strength of the alginate hydrogel can also vary from one alginate to another. For example, following a careful extraction procedure, *Laminaria hyperborea* gives strong gels, while *Laminaria digitata* gives a soft-to-medium strength gel.<sup>4</sup> Bacterial biosynthesis may provide alginate with more defined chemical structures that can be obtained from seaweed-derived alginate.<sup>5</sup> Generally, alginates with a low M/G ratio will give a stronger gel.

Alginate possesses several essential properties that make it suitable for use in HVTE. The first property is its ability, when dissolved, to increase the viscosity of aqueous solutions, which is particularly important in formulating extrudable mixtures for 3D printing. The second property is its ability to form gels in mild conditions, for example by adding calcium salt to an aqueous solution of alginate. Calcium cations displace sodium from alginate and bind long-chain alginate molecules together, resulting in the formation of a hydrogel. This property is a basis for reactive extrusion and inkjet printing-based solid free-form fabrication.

Unlike agar gels where the water must be heated to about 80°C to dissolve the agar and the gel forms when cooled below about 40°C, the alginate hydrogel requires no heat for its formation; moreover, the gel does not melt when heated. The ionically triggered gelation of alginate is chemo-reversible while covalent cross-linking is permanent, and, therefore, it is possible to modulate degradation rates and mechanical stiffness.<sup>6,7</sup>

The next fundamental property of alginate is its ability to form films,<sup>8,9</sup> fibers,<sup>10–12</sup> beads,<sup>13</sup> and virtually any shape in a variety of sizes. Moreover, as the partial oxidation of alginate does not significantly interfere with its gel-forming capability, its customized degradation could be induced by periodate oxidation of the alginate backbone.<sup>14</sup>

Within the field of biomedicine, there is a broad scope for the application of alginate including wound healing, cell transplantation, delivery of bioactive agents, such as chemical drugs and proteins, heat burns, acid reflux, and weight control applications.<sup>1,15</sup> Recently, alginate-based biomaterials used in the treatment of myocardial infarction have entered into the advanced stage of clinical trials.<sup>16,17</sup> In human studies,<sup>16</sup> implementation of alginate within the ventricular muscle wall has been shown to reduce the wall stress of the dilated heart and relieve the muscle tension.<sup>16</sup> With the similar strategy, the aqueous mixture of sodium alginate and calcium gluconate has been used as a bioabsorbable cardiac matrix to prevent negative ventricular remodeling following acute myocardial infarction.<sup>17</sup> During the standard catheterization procedure, the hydrogel is injected into the damaged heart muscle via the coronary artery. The injected material perfuses and polymerizes the sites between the cells and fibers of the damaged tissue. The hydrogel content provides the necessary physical support to the heart muscle during repair and recovery.

In a review by Ruvinov and Cohen,<sup>18</sup> alginate is described as a material of non-thrombotic nature, which is confirmed by numerous alginate medical applications and its use in clinical trials. However, there is a lack of direct confirmation in the literature to support this opinion, probably because “evidence of absence” is hard to present. For this reason, we investigate this matter more extensively.

For example, Cabrales *et al.*<sup>19</sup> used alginate as a plasma expander to maintain perfusion and plasma viscosity during extreme hemodilution. They found no incidence of thrombosis when alginate (0.7% w/v) together with dextrans and other components were injected into the bloodstream of hamsters. However, they did not eliminate the possibility that dextrans hindered thrombosis of alginate.

Duncan *et al.*<sup>20</sup> monitored the fate of alginate following intravenous administration in mice. At 24 h after intravenous administration, they found that the low-molecular-weight fraction of the injected polymer was excreted in the urine and that the larger polymer fraction remained in the circulation, which did not readily accumulate in any of the tissues. In the case of thrombosis, the accumulation of alginate would be a reasonable scenario.

Furthermore, Leor *et al.*<sup>21</sup> investigated the effect of intracoronary injection of the alginate hydrogel on reversing left ventricular remodeling in swine. Examination of the heart following injection showed that alginate was deposited as the hydrogel in the infarcted tissue. Importantly, the intracoronary injection of alginate into a healthy heart showed no evidence of intravascular thrombi.

More direct evidence on non-thrombotic nature of alginate was provided by Goe *et al.*<sup>22</sup> Among others parameters, researchers compared platelet adhesion to native and modified polyvinyl chloride (PVC) surfaces. Surface modifications included covalent bonding of sodium alginate, heparin, and sodium alginate/heparin composites. Alginate modification caused a fourfold reduction in platelet adhesion compared with unmodified PVC. A reduction in the platelet attachment by a factor of 10 was observed for PVC surfaces treated with a sodium alginate/heparin composite compared with untreated PVC. This result set the comparison scale; however, more work is needed to estimate the influence of cross-linking on the thrombogenicity of alginate.

Based on the above-cited publications, it can be stated that the non-thrombogenic nature of alginate has made it an attractive candidate for cardiac applications,<sup>23–25</sup> including scaffold fabrication for HVTE.<sup>26</sup>

Solid free-form fabrication techniques supporting biomedical applications of alginate can be realized through two technologies: inkjet-based and extrusion-based systems. Both methods enable the production of scaffolds for cell encapsulation that increases the seeding efficiency of fabricated structures.

### 3. GENERAL CHARACTERISTICS OF THE AORTIC HV AND SCAFFOLD REQUIREMENTS

The aortic HV (AHV, see Figure 1) is responsible for the unidirectional blood flow between the left ventricle and the aorta. It is a highly demanding environment where the valve opens over 100,000 times each day, and is subjected to shear stress, bending forces, strain, and loading forces.<sup>27</sup> While most humans will have a normal valve function, some will need AHV replacement surgery due to several problems such as sclerosis, stenosis, and aortic aneurysm. It has been estimated that by 2050, the annual number of patients requiring HV replacement worldwide will be about 850,000.<sup>28</sup>

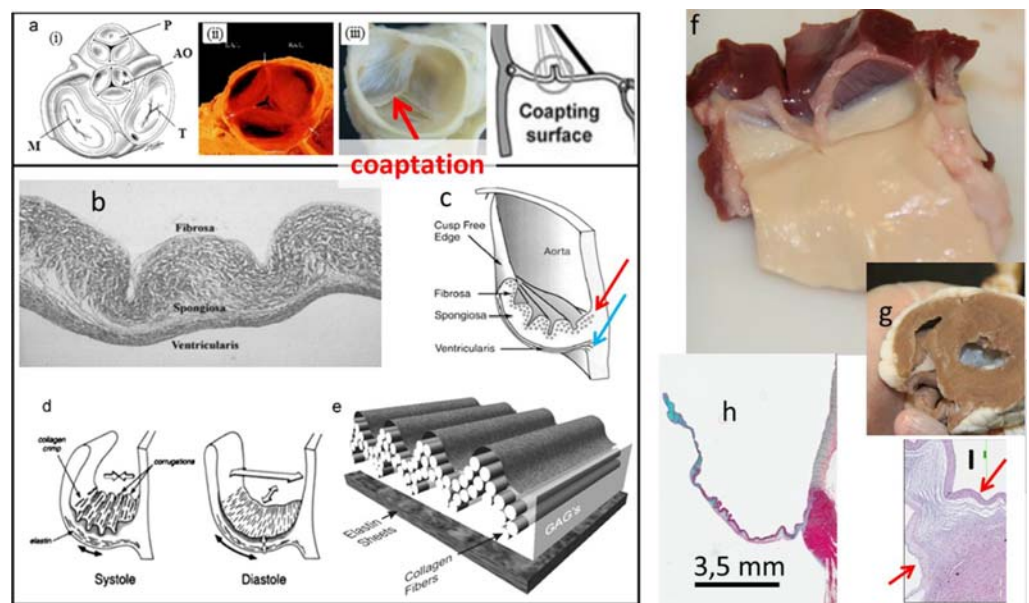


**Figure 1.** (a) The basic functional/structural aspects of the HV. (i) Schematics of the 2D position of the four valves on the valvular basal plane of the heart, where P: pulmonary valve, AO: aortic valve, M: mitral valve, and T: tricuspid valve, (ii) porcine pulmonary HV, and (iii) decellularized porcine AHV. (b) Leaflet consists of three individual layers: fibrosa, spongiosa, and ventricularis. (c) Each layer contains specifically oriented fibers. The red arrow indicates circumferentially oriented fibers of collagen. The blue arrow indicates radially oriented fibers of elastin. (d, e) The types (collagen, fibronectin, elastin) and arrangement of fibers are responsible for the function of the valve (opening and closing). (f) The fibrosa layer is a continuation of the aorta, and ventricularis is a continuation of the ventricular channel. (g) The view of the sheep aortic valve from the ventricular side, after dissecting the heart. (h) The leaflets contain glycosaminoglycans (mainly in spongiosa, blue color), which works as a lubricant between layers, and shock absorber. (i) Histology of the hinge area (between the arrows) highlights the importance of fiber arrangement. The cells are hosted and maintained by a highly organized network of fibers. Figures (a)–(e) were reprinted with permission from.<sup>33</sup>

Currently, the valve is replaced with a mechanical or bioprosthetic valve. The problem with these kinds of replacement is that the patient will need to be on lifetime anticoagulants (mechanical valves), whereas bioprosthetic valves are limited to tissue degradation. An alternative that has been widely studied is the use of a biodegradable scaffold that has a mechanical integrity close to the aortic valve, where the cells can grow and remodel the structure and the final product will be a functional autologous aortic valve.<sup>29,30</sup>

This scaffold must be able to mimic the complexity of the AHV. One significant feature of the AHV is its ability to interact with its constituent parts through passive and active communications and adjust the appropriate response to the environment.<sup>31</sup> A passive communication can be seen during the changes in the sinuses upon establishing the vortices that ensure valve closure, preventing blood backflow and coronary flow during systole.<sup>27</sup> Examples of active communication are changes in the

shape, size, and stiffness of the cusp, annulus, sinus, and sinotubular junction during specific parts of the cardiac cycle.<sup>32</sup> Thus, to achieve this complexity, the substitute scaffolds must host cells that will be able to be housed, and produce an extracellular matrix (ECM) that will function in a similar way to the native valve.

An important role of the scaffold is to provide a temporary 3D structure for cellular attachment, infiltration, and proliferation. The materials should possess biomimetic properties and should be highly porous, thereby facilitating cellular infiltration, stimulation of neo-tissue formation, and integration with native tissue.<sup>34</sup> The scaffold should be non-immunogenic, capable of attracting, housing, and instructing cells to produce the specific phenotype.<sup>35</sup> It must also reproduce the performance and mechanical properties of the native valve in both the short and long terms. As the target geometry of the AHV, tissue engineers use a simplified model of the native valve (see Figure 2, bottom panel).

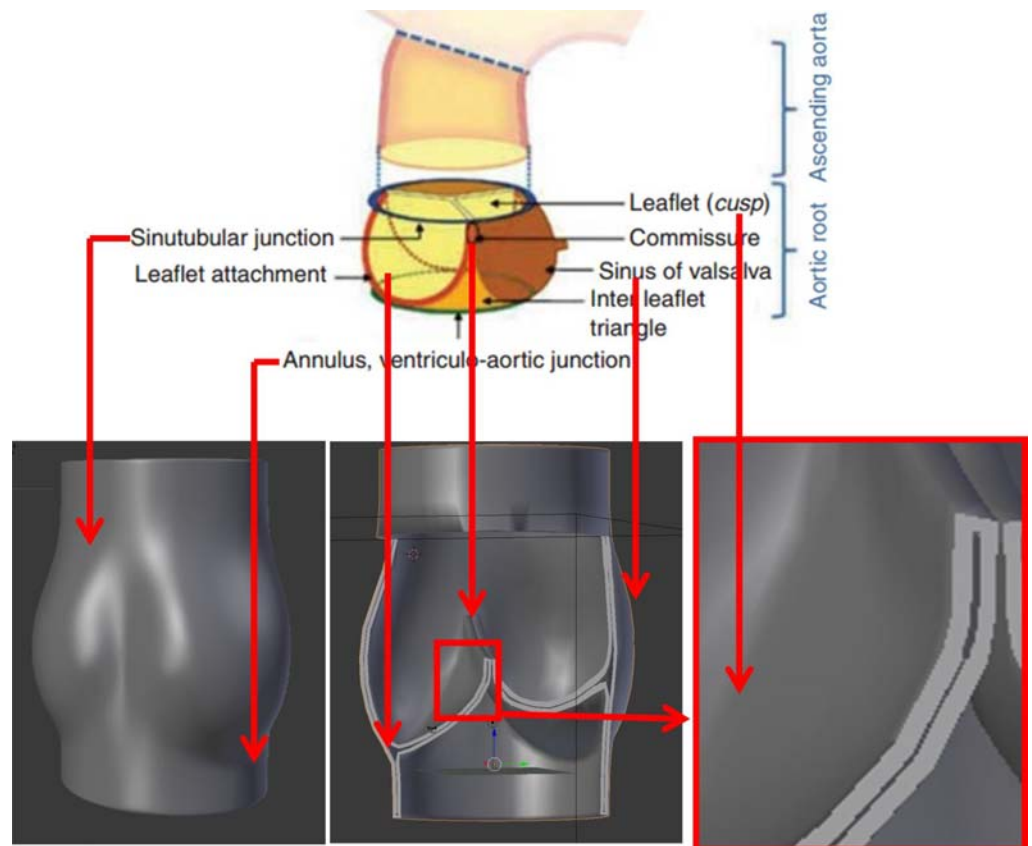


**Figure 2.** The geometry of the native AHV (top) and scaffold (bottom). The top panel was reprinted with permission from <sup>27</sup>.

#### 4. 3D PRINTERS SUITABLE FOR ALGINATE DEPOSITION – THE ROLE OF OPERATOR

There are two opposing approaches in 3D printing technologies. The first category of devices includes printers working with only specific materials, usually delivered from manufacturers in ready-to-use form. The material is customized to work with a given device. An example of such printer is Objet Eden260VS – 3D printer (Stratasys, Edina, Minnesota, USA). This equipment operates with several types of cartridges consisting of inkjet printable, photocurable monomers yielding stiff or elastic, white, black or semi-luminal objects. The involvement of the operator in printing is limited. The process is as complex as printing a paper document in the standard desktop printer. Due to the compatibility of ink and its dispensing mechanism, the resolution of printing is high and an object with many details can be obtained (see Figure 3 to compare CAD design with printed HV).

Conversely, a considerable amount of work is usually involved in preparing the ink and optimizing the printing parameters for hydrogel deposition, especially when the cells are part of the formula. In the extrusion-based technique, the printer is, in fact, a syringe attached to a programmable XYZ positioning

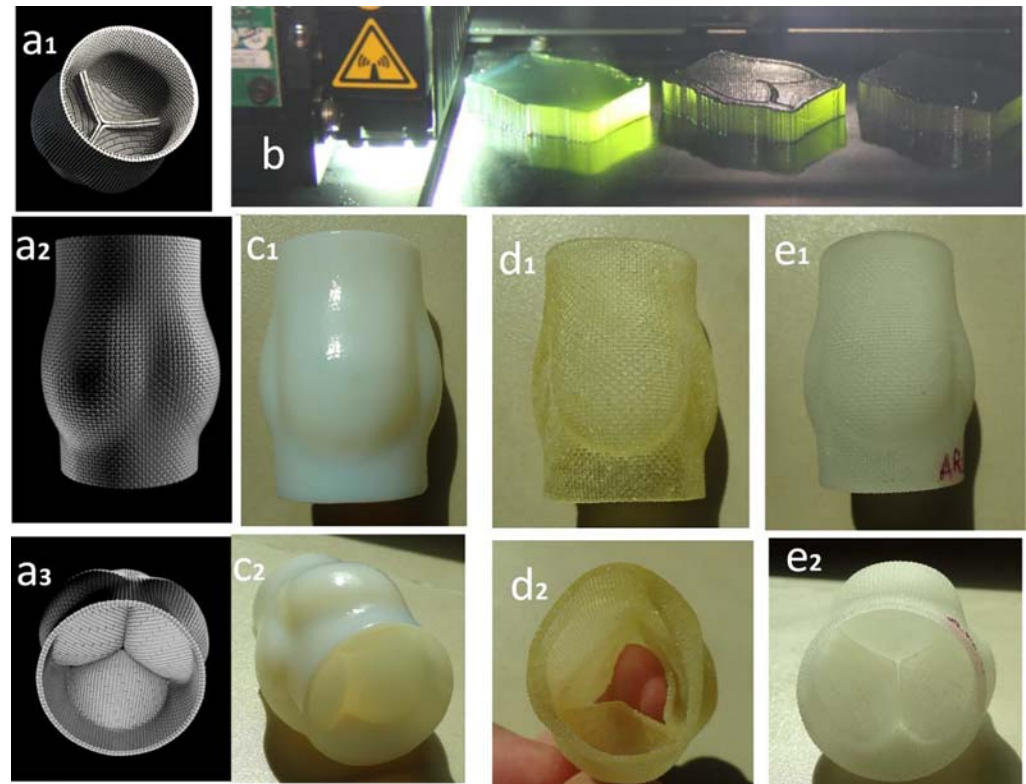


**Figure 3.** Examples of HVs printed using Objet Eden260VS – 3D printer (Stratasys, Edina, Minnesota, USA) by inject printing light-curable acrylate monomers. The diameters of the bases of the root are 28 mm. (a<sub>1</sub>–a<sub>3</sub>) CAD-designed geometries of HV. (b) Three half-way printed valves. Cross-sections of the valve are filled with support material. HV printed in white, stiff polyacrylate, view from (c<sub>1</sub>) the side and (c<sub>2</sub>) ventricular side. HVs made out of (d<sub>1</sub>–d<sub>2</sub>) flexible semi-luminal and (e<sub>1</sub>–e<sub>2</sub>) rigid semi-luminal polyacrylates. Both are provided with the texture-mimicking surface of woven fabric. The printer is not suitable for direct printing of the alginate structure; however, it yields an elastic and firm object with high precision (only minor operator involvement is required).

platform. The freedom of choosing the printed material is accompanied by reduced speed and precision of printing. The basic parameters that need to be adjusted for a given formulation include the width and height of the path as well as the speed of the path deposition. For example, a printing solution with a low concentration of alginate will generate wide but low paths; on the contrary, a high concentration of alginate may yield narrow but high paths. The particular parameters of the paths need to be estimated and fed to the printing system to avoid gaps or material overprinting in the structure. Usually, the trial-and-error method is the only solution for parameter optimization, so the printer operators' experience plays a pivotal role in organizing the experiments. Nevertheless, useful tips may be found in the literature. For example, Kang *et al.*<sup>36</sup> conducted a study on quantitative optimization of solid free-form deposition of aqueous hydrogels. In this interesting work, a set of standard methods and parameters for monitoring both the precision and resolution of Fab@Home-mediated 3D printing were described. Porcine aortic valve interstitial cells (PAVICs) were used as a model cell type to assess cell viability. Printing conditions did not affect PAVIC viability within the ranges applied. However, the pressure, path space, and path height all significantly affected print resolution and accuracy. Based on this work, the optimal extrusion parameters yielding accurate 3D geometries could be predicted.<sup>36</sup> Further work reported from Cohen *et al.*,<sup>37</sup> revealed the importance of mixing the ingredients before extrusion, which improves hydrogel homogeneity and the quality of 3D-printed constructs.

### 5. 3D PRINTING OF ALGINATE USING INKJET-BASED TECHNIQUES

Inkjet printing is a process in which droplets of ink extruding from nozzles are directed onto a substrate.<sup>38</sup> Boland *et al.*<sup>39</sup> used the inkjet-based technique to construct biodegradable synthetic scaffolds. They filled the ink cartridge with calcium chloride (CaCl<sub>2</sub>) and sprayed on an underlying alginate acid solution to form biodegradable hydrogel scaffolds. The divalent cations promoted the

cross-linking of individual negatively charged alginic acid chains, resulting in a 3D network structure. By spraying cross-linkers onto ungelled alginic acid, hydrogels with controlled microshell structures were built under mild conditions (see Figure 4). Endothelial cells were attached to the inside of these microshells and remained viable in constructs as thick as 1 cm due to the programmed porosity. Models with mechanical properties matching cardiac tissue were developed based on a finite-element modeling and computer-aided design (see Figure 4a). In this study, there were two major concerns related to alginate-based HVTE. First, the relatively complex architecture of the object was obtained; perhaps the same technique could be adapted to develop the HV. The second important concern is the encapsulation of endothelial cells, which was successfully used for HVTE by other authors.<sup>40</sup>

Geometrically the same structure was used by Boland *et al.*<sup>39</sup> to fabricate functional 3D tissue constructs by arranging alternate layers of mammalian cardiac cells and biocompatible alginate hydrogels, according to predesigned 3D patterns. The printed scaffolds demonstrated adequate elastic moduli and tensile strengths for harmonic responses to cardiomyocyte contractility.<sup>41</sup> It may be especially useful to recreate the trilaminar layer architecture of HV leaflets.

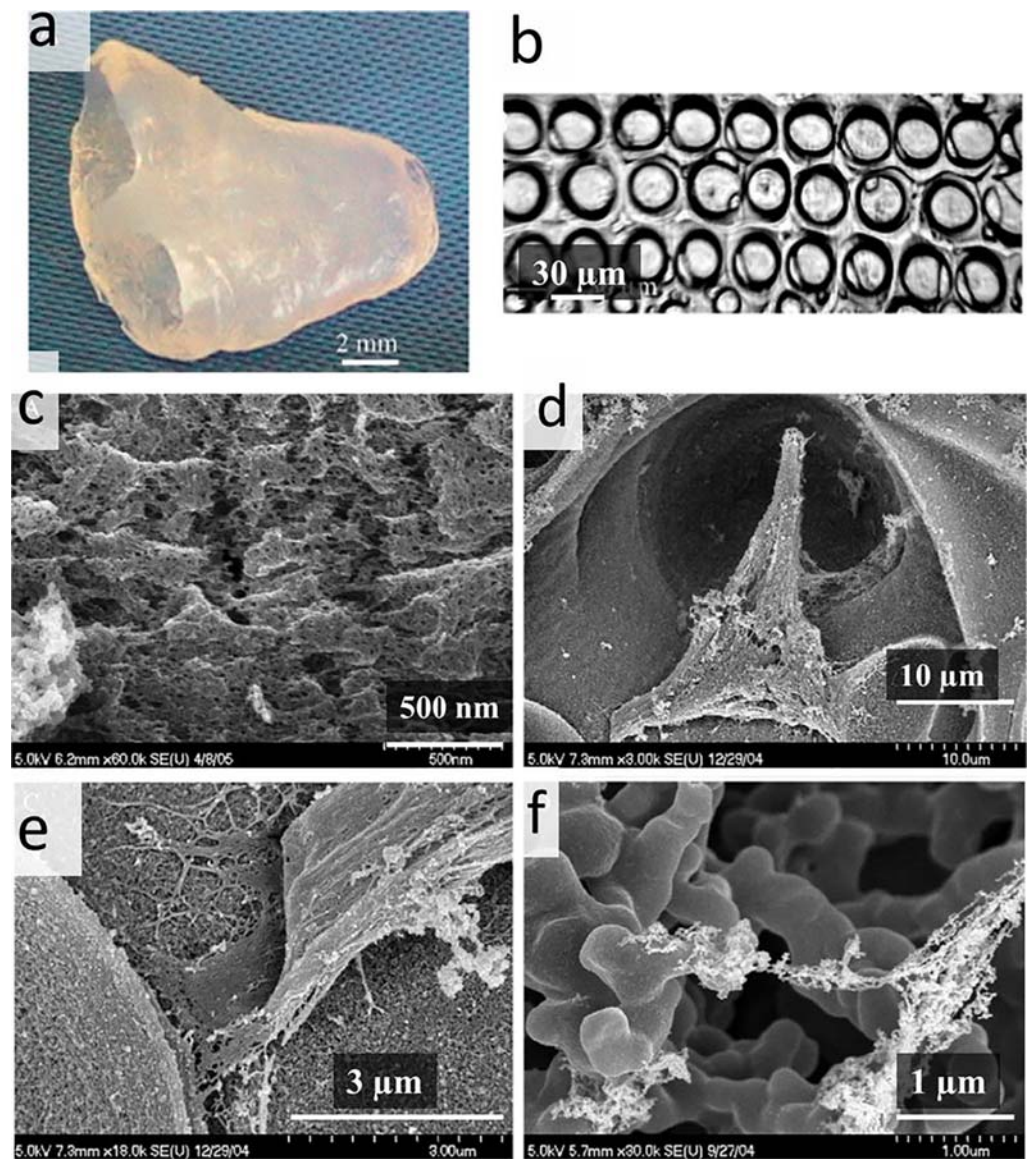


**Figure 4.** (a) Macroscopic and (b) microscopic views of inkjet-printed alginate structures generated by Boland *et al.*<sup>39</sup>. (c–f) SEM micrographs of endothelial cells attached to alginate shells. (c) Shell wall shows nanosized pores in the alginate. (d) An endothelial cell is shown to be attached inside an alginate shell. (e) Filopodia and lamellipodia, typically involved in cell motility, are observed to be interacting with the alginate material. (f) Fibrous secretion is shown to be interacting with alginate. Reprinted with permission from <sup>39</sup>.

In the context of HVTE, the drawback of the aforementioned strategies is construct saturation with calcium, which may affect calcium-dependent signaling pathways of the cells and, in the longer term, may enhance the calcification of cardiac tissues.<sup>42</sup>

Some may argue that alginate and its cross-linker would be eluted and its role will be taken over by cell-secreted ECM proteins before calcification. Nevertheless, to eliminate calcium-related risk, other divalent cations such as  $Zn^{2+}$ ,  $Ba^{2+}$  and  $Sr^{2+}$  may be inkjet-printed as cross-linking agents,<sup>43,44</sup> after estimating their cytotoxicity at a given concentration.

Inkjet printing of a complex multi-component construct, which is required in HVTE, is not straightforward. An alginate substrate would need to be frequently and comprehensively exchanged to seed valvular endothelial cells and valvular interstitial cells (VICs) within the structure alternately. Moreover, to avoid casual cell mixing, the construct would need to be washed to remove one type of cells before implementing another one. A solution to this limitation that potentially enables quick fabrication of multicellular HV-like structures was proposed by Arai *et al.*<sup>45</sup> In this case, to fabricate 3D gel structures, the cell-suspended sodium alginate solution was inkjet-printed onto an underlying  $CaCl_2$  solution. Alginate beads (80  $\mu m$  in diameter) were assembled layer by layer into pyramid-like objects. There is a favorable match between the CAD design and the final structure; however, it would not be feasible to obtain the HV geometry in a method proposed by Arai *et al.*<sup>45</sup>, as the HV structure would collapse without a support material during printing. Furthermore, the university logo mark was fabricated by three-layer lamination (see Figure 5).<sup>45</sup> 3D inkjet biofabrication of images has a particular importance for HVTE, as it is the first step for 3D printing governed by data obtained from magnetic resonance imaging and X-ray computed tomography.<sup>46</sup>

Another Japanese group used the same strategy to inkjet print 3D biological structures composed of alginate hydrogels and living cells. The structures were printed with much enhanced precision and resolution as the performance of the inkjet nozzle was optimized for hydrogel deposition.<sup>47</sup> Drops with diameter  $< 25 \mu m$  were generated. The printing parameters were further optimized to obtain single

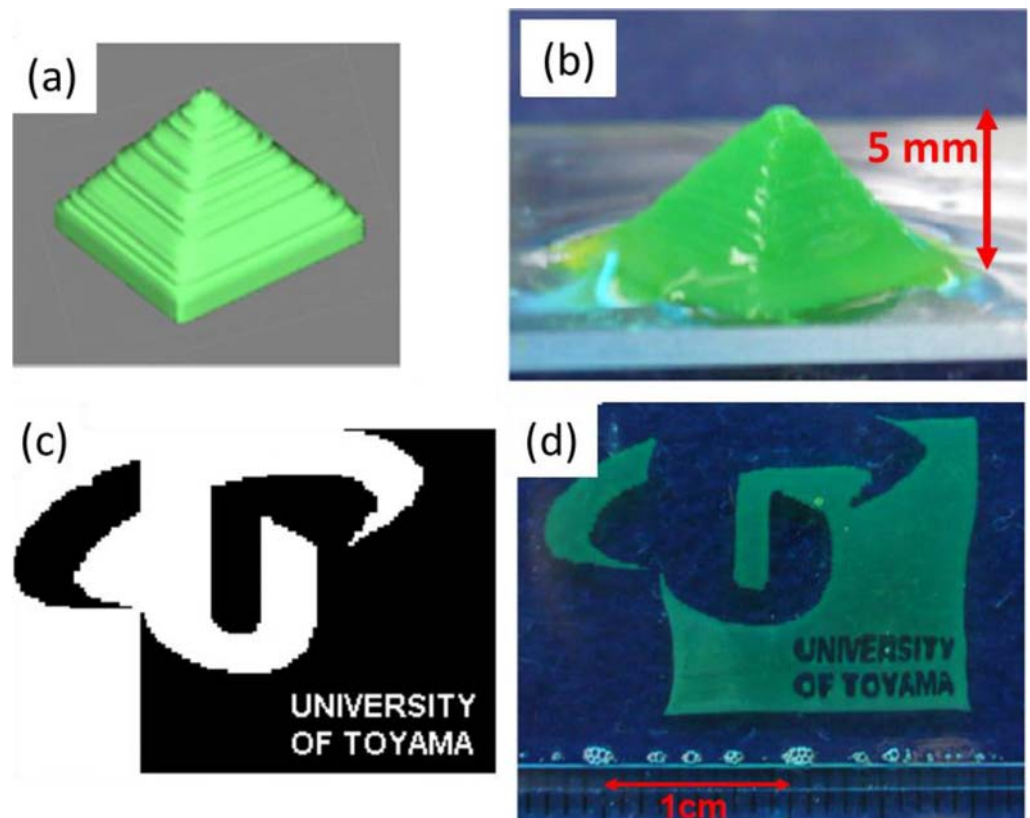


**Figure 5.** (a–d) CAD models and photographs of the inkjet-printed structures. Samples of 3D alginate hydrogels. (a) 3D computer model of a pyramid structure. (b) Fabricated 3D pyramid structure obtained by inkjet printing cell-suspended alginate. (c) Logo mark image. (d) Fabricated logo mark of three-layer lamination obtained by inkjet printing cell-suspended alginate. Reprinted with permission from <sup>45</sup>.

HeLa cell-laden beads. Subsequently, the beads were patterned and assembled into 3D structures such as tubes and sheets (see Figure 6), which are highly relevant to the structural features of the HV architecture, as shown in Figure 1. For example, printing the hydrogel in the form of a spiral tube may yield structures with similar elasticity to the ventricularis.

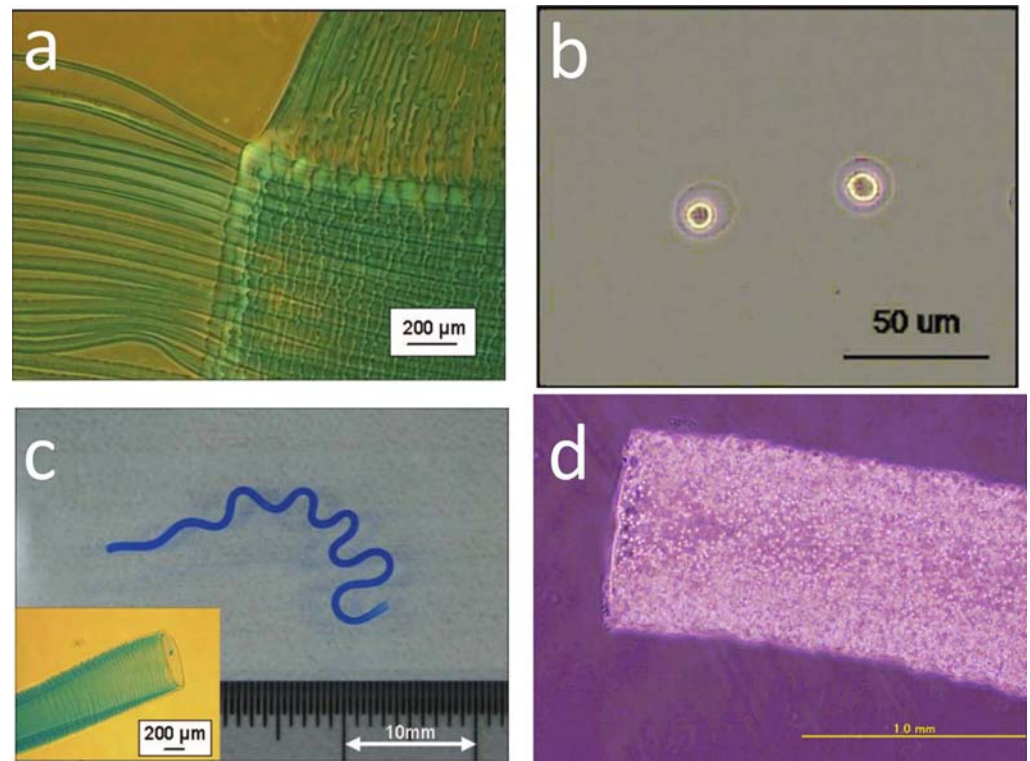


**Figure 6.** Macroscopic and microscopic views of inkjet-printed alginate structures generated by Nishiyama *et al.*<sup>47</sup>. (a) Alginate gel lamination: the threads of alginate were combined, thanks to the optimization of the nozzle head speed and ejecting frequency. (b) Alginate beads including one HeLa cell per bead. (c) Gel tube with an enlarged view of the opening at the tip of the tube. (d) Alginate tube with HeLa cells. Reprinted with permission from <sup>47</sup>.

Furthermore, printing with single-cell precision is a very attractive feature for HVTE applications. Three distinct layers of the HV are interconnected, thereby preventing delimitation. Controlling the interpenetration of cells by printing them with high precision potentially enables the optimization of the interaction between the layers of HV leaflets.

This single-cell precision in the cell deposition process has not yet been reported by any other technique.<sup>48</sup> Given the potential of inkjet printing for operating in a high-throughput manner, this technology holds much potential for further development.<sup>47</sup>

### 6. 3D PRINTING OF ALGINATE USING EXTRUSION-BASED TECHNIQUES

A considerable amount of literature has been published on the extrusion-based fabrication of 3D scaffolds for tissue engineering. The extrusion-based systems often require melting of deposited materials and involve an elevated temperature that is undesirable from the perspective of scaffold bioactivity. Several techniques that overcame this limitation were proposed (see Figure 7) to process alginate and other hydrogels.<sup>49,50</sup>

The shape of 3D structures (see Figure 7) that summarizes research on 3D printing of alginate using the extrusion method is not a random choice. Grids play a pivotal role in the quality control for the 3D deposition process. It can be used to optimize the printing parameters and to estimate whether the extruded formulation will be suitable for producing objects with desired precision and complexity. Since the spaces between the vertical and horizontal columns of the gel can be easily measured and homogeneity of printed patterns can be quantified, the grids can also be used to estimate the effect of

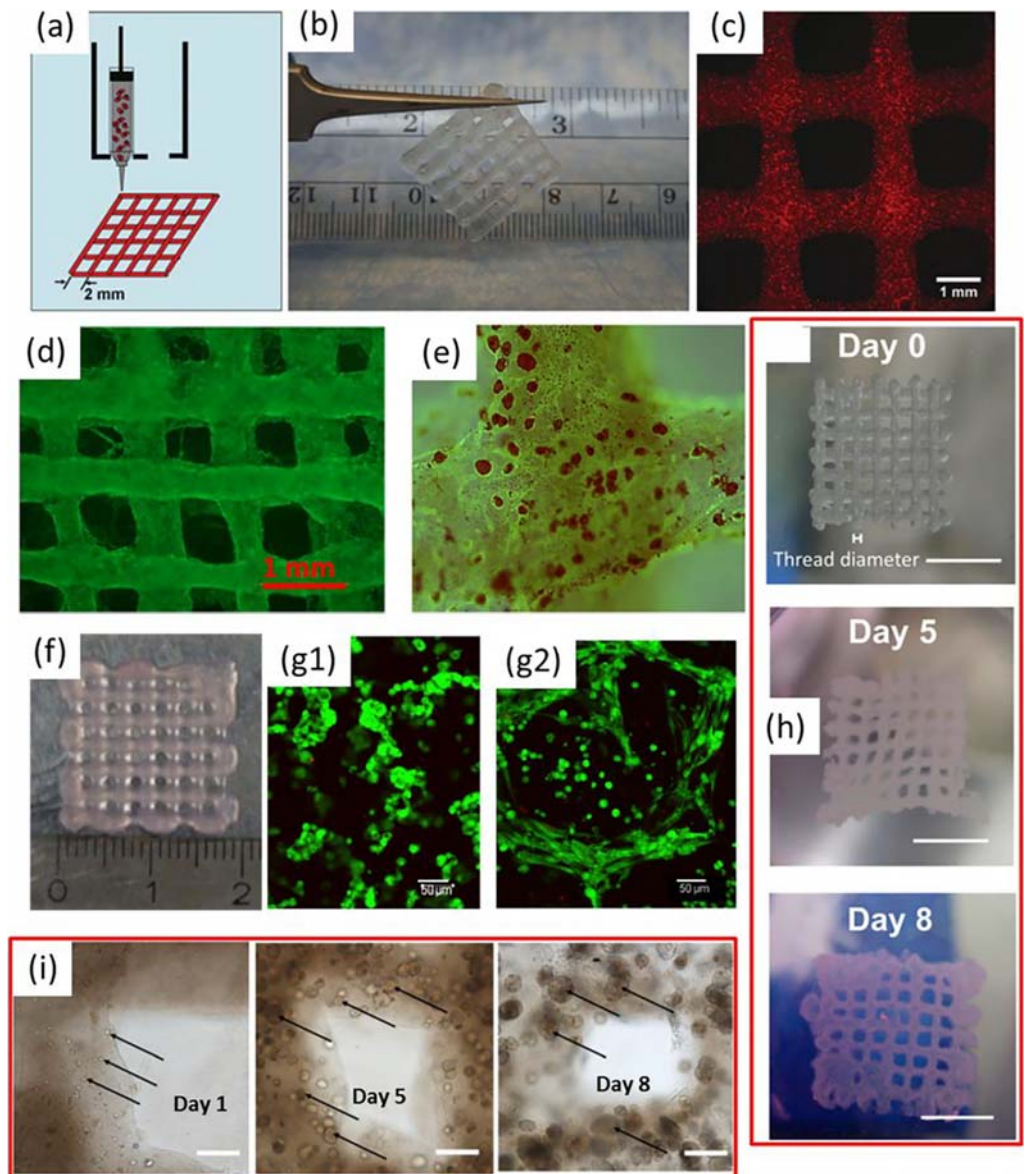


**Figure 7.** Bioprinting of 3D grid pattern structures. (a) Schematic of the bioprinting process with a single cell type and single syringe. (b) Alginate/gelatin hydrogel structure bioprinted after ionic cross-linking. (c) Fluorescent image of a printed grid with encapsulation of a cell tracker red-labeled VICs. Reprinted with permission from <sup>26</sup>. (d) Adipose-derived stromal (ADS) cells encapsulated in the 3D structure, cultured on a plate, immunostained against CD34<sup>+</sup> (ADS cells and endothelial cells indicated in green). (e) ADS cells in the 3D structure controlled to differentiate into endothelial cells (green) and adipocytes (red). Reprinted with permission from <sup>51</sup>. (f) Printed human cardiomyocyte progenitor cells (hCMPCs) in 10% alginate scaffold. Confocal analysis of live/dead assay of printed hCMPCs in (g1) unmodified and (g2) RGD-modified alginate scaffolds after two weeks of culture. Reprinted with permission from <sup>52</sup>. (h) Top view of 3D HeLa/hydrogel constructs on days 0, 5 and 8. Scale bar: 5 mm. (i) HeLa cells in 3D HeLa/hydrogel constructs observed by using a phase-contrast microscope on days 0, 5 and 8. Scale bar: 200  $\mu$ m. Black arrows indicate cells and cellular spheroids in the 3D construct. Reprinted with permission from <sup>53</sup>.

cell encapsulation and proliferation within the construct (shrinking, swelling). Moreover, the interaction of the extruded material on junctions determines how layer-by-layer deposition may be arranged to yield 3D objects. In fact, grid printing is a starting point for most of the free-form fabrication projects. Therefore, it is important to summarize how researchers present this basic step of their process, which, for the novice, can be trivial. Even if the final target achieves a structure as complex as HV,<sup>26</sup> the first step is to print a grid (see Figure 7a–c).

Xu *et al.*<sup>41</sup> demonstrated an approach in which a blend of sodium alginate, gelatin, fibrinogen, and cells was networked by the stepwise cross-linking of sodium alginate with a  $\text{CaCl}_2$  solution and fibrinogen with a thrombin solution. Gelatin was blended as a co-material that served to provide solution-to-gel phase transition during the fabrication process. Researchers demonstrated that within the structure, adipocytes and  $\beta$ -cells, (obtained by *in situ* differentiation of ADS cells) constituted the adipo-insular axis that regulates energy metabolism. The derived 3D model of the disorder was found to cover most of the physiological and pathological features of the metabolic syndrome. As shown in Figure 7d, e, ADS cells encapsulated in the 3D structure can be *in situ* differentiated into endothelial cells (green).<sup>51</sup> For HVTE, this work is essential for a few reasons. First, other researchers showed that ADS cells sense mechanical stimulation and produce collagen and elastin, which has positive implications for HVTE.<sup>54</sup> Another advantage is that ADS cells can be isolated from a patient's tissue.<sup>55</sup> Moreover, ADS cells that can be *in situ* differentiated into endothelial cells may also be used for recreating cellular components of the HV.<sup>40,56</sup>

It is acknowledged that unmodified alginate does not support cellular proliferation.<sup>15</sup> Therefore, to investigate whether cellular proliferation in alginates may be enhanced, the tissues constructed with alginate and RGD-modified alginate were compared. The differences in cell morphology were distinct after one week of culture. More elongated cells were observed in the RGD-modified alginate scaffold, while in the unmodified alginate, the cells were mostly organized in spheroid-like structures (see Figure 7g). This previously reported phenomenon clearly demonstrates the differences in the affinity of alginate-based hydrogels to support cellular proliferation.<sup>10</sup> Tissue engineering strategies involving these affinity differences in the complex 3D cellular patterning are overlooked and not yet reported in the literature. In the future, by alternating alginate with its modified derivatives during layer-by-layer deposition, it may be possible to precisely govern the cellular growth within the 3D structure. For HVTE, it could be an extremely powerful tool, especially with regard to the smart scaffold strategy. The smart scaffold is implemented in patients without cells and must recruit the host patient's cells.<sup>28</sup> In this case, providing the structure with hydrogels of different cellular affinity would potentially help guide the cells to predetermined locations. For example, a subset of endothelial progenitor cells can be transferred by hydrogel channels to spongiosa and can differentiate inside the leaflet, differently from the other cells located on the surface of the leaflet.

The mixture of alginate, gelatin, and fibrinogen was used by Zhao *et al.*<sup>53</sup> to create a cervical tumor model. A fibrinogen/HeLa mixture, gelatin solution, and sodium alginate solution were mixed and drawn into a syringe, from which the mixture was extruded in a layer-by-layer fashion at  $10^\circ\text{C}$ , followed by alginate and fibrinogen cross-linking with  $\text{CaCl}_2$  and thrombin, respectively. Then, matrix metalloproteinase activity, chemo-resistance, protein expression, and cell proliferation were measured. The results revealed that the 2D planar cell culture models had significantly less simulated tumor characteristics than the printed 3D models.<sup>53</sup> Figure 7h shows how changes in the dimensions of the 3D-printed grid may be used to monitor cellular growth and scaffold degradation in time. On the other hand, Figure 7i shows the typical behavior of cells within unmodified alginate, where the single-cell suspension is transformed into clump suspension over time. Perhaps increasing the initial concentration of cells would enhance clump interconnectivity. Therefore, the significance of this paper for HVTE also lies in measuring the chemo-resistance of cancer cells in a 3D environment. The culture of any cells *ex vivo*, including those constituting the HV, carries a risk of mutation because the cells grow away from the protection of the recipient's immune system. From this perspective, the incorporation of an anticancer drug into alginate hydrogels may be necessary for eliminating or preventing the occurrence of mutated cells within the construct.

A low-temperature deposition strategy was used by Li *et al.*<sup>57</sup> to assemble multiple cells and ECM materials in a single construct. ADS cells were combined within an alginate/gelatin/fibrinogen hydrogel to form a vascular-like network and hepatocytes combined with gelatin/alginate/chitosan were placed around it. The construct was stabilized in a  $\text{CaCl}_2$ /thrombin/ $\text{Na}_5\text{P}_3\text{O}_{10}$  solution after the assembly was complete. Subsequently, the ADS cells were induced to differentiate into endothelial-like cells with an endothelial growth factor to mimic vascularization of a liver-like structure.<sup>57</sup> This example is important for HVTE since recruited and/or encapsulated pluripotent cells need to be specialized in a mature construct. This process may be triggered by including growth factors as in the example discussed above.

Gaetani *et al.*<sup>52</sup> described the example of tissue engineering that involves hCMPCs. To generate *in vitro* tissue with homogeneous distribution of hCMPCs in the scaffold, sodium alginate was

dissolved in the culture medium, cells were added, and the solution was printed using the 3D tissue printer BioScaffolder (GeSiM, Grosserkmannsdorf, Germany). After printing, the tissues were incubated with  $\text{CaCl}_2$  in  $\text{H}_2\text{O}$  and 0.1% FBS to allow the polymerization of the cell/alginate constructs. While the geometries of the constructs were simple (patches), the authors wisely used it to optimize alginate concentration and construct porosity to maximize the viability of the encapsulated cells. After printing, it was determined that 92 and 89% of the cells were viable at one day and one week of culture, respectively. Importantly, printed hCMPCs had not only retained their commitment to the cardiac lineage, but also the expression of the early cardiac transcription factors and the sarcomeric protein TroponinT (cardiac differentiation markers) was enhanced in the 3D culture when compared with the 2D culture. Moreover, from the perspective of HVTE, the authors noted a very crucial property of the alginate-based cell encapsulation system, namely its capacity to enable cell migration out of the alginate matrix into surfaces with larger cell attachment affinity. Printed hCMPCs were able to migrate from the alginate matrix and colonize a matrigel layer, thereby forming tubular-like structures, after three weeks of culture. It indicated that alginate could be used as a sacrificial cell delivery vehicle while retaining the functional properties of the cells and supporting their viability. As mentioned above, calcium-containing alginate hydrogels may be linked with valvular calcification. Thus, the fact that alginate may be dispensed in the process of construct maturation is critical to its application in HVTE.

To create 3D branched vascular systems, Huang *et al.*<sup>58</sup> developed a hybrid hierarchical polyurethane (PU)-cell/hydrogel construct by a double-nozzle low-temperature deposition method. PU was used as an external scaffold material to provide mechanical support, while the alginate/gelatin/fibrinogen hydrogel was used as an internal scaffold material for the accommodation of ADS cells. After fabrication, the 3D composite construct was thawed at room temperature and cross-linked/polymerized. The construct was cultured under static or dynamic conditions, showing stable architectures and excellent biocompatibilities. It is known that molecular segments of PU can be tuned to obtain specific mechanical properties of the polymer.<sup>59</sup> Therefore, together with alginate, PU may be able to provide distinct mechanical properties to specific regions of the HV while retaining cell hosting capacities.

Another interesting method used for the direct free-form fabrication of cell-seeded alginate hydrogels in arbitrary geometries was described by Cohen *et al.*<sup>60</sup> (see Figure 8). The authors used calcium sulfate ( $\text{CaSO}_4$ ) as a cross-linking agent for the alginate hydrogel to produce pre-seeded living implants. Due to its lower solubility, calcium sulfate can slow the gelation rate and extend the working time of alginate gelation. Alginate hydrogel was mixed and loaded into a syringe and allowed to cure for 10 min before extrusion. This step increased the viscosity of the hydrogel that enabled a more accurate deposition. Moreover, deposited layers of alginate merged efficiently due to the longer

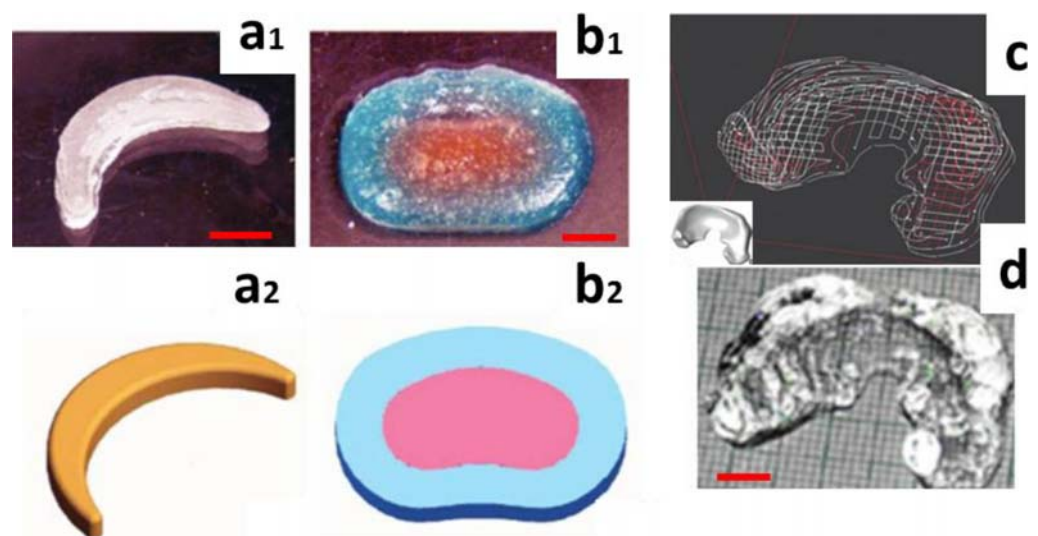


**Figure 8.** CAD models and photographs of extruded samples of 3D alginate hydrogels. (a<sub>1</sub>) Single and (b<sub>1</sub>) multi-material constructs made by reactive extrusion of alginate and (a<sub>2</sub>, b<sub>2</sub>) their corresponding CAD models. (c) The layout of extrusion paths generated with trajectory planning software. (d) Spatially heterogeneous construct based on (c), made by reactive extrusion of alginate. Scale bars: 1 cm. Reprinted with permission from <sup>60</sup>.

cross-linking time provided by  $\text{CaSO}_4$ . The process was determined to be sterile and enabled high cell viability (over 90%). The constructs were used for *in situ* repair of osteochondral defects. As mentioned previously, to be functional, the HV must contain a specific anisotropy of the fibril ECM, which can be triggered by instructing the cells to grow in an oriented manner. Slowing down the alginate cross-linking by applying a less soluble salt of calcium enables the deposition of highly viscous alginate blends. The extruded columns could preserve its fundamental cylindrical geometry. By altering cell-laden and cell-free threads, the lengthwise migration of the cells can be enforced, leading potentially to oriented ECM deposition.

Based on the study by Cohen *et al.*<sup>60</sup>, the match between the CAD models and photographs of extruded samples of 3D alginate hydrogels can be estimated (see Figure 8). Considering that scale bar as 1 cm, the precision of printing demands for improvement. Figure 8c shows the layout of extrusion paths generated with the trajectory planning software. This aspect is an important point of consideration for HVTE. As anisotropy of the fibril structure of the HV is a critical factor for its performance, the paths of the material deposition should be planned to follow the anisotropy. For example, by altering the extrusion of cell-free and cell-laden alginate threads, it allows us to impose the cellular growth in an oriented manner as the migration of cells lengthwise will be preferential over the cross-thread migration.

Other researchers have found that the 3D structure can be efficiently plotted by alternating layers of alginate and/or poly( $\epsilon$ -caprolactone) (PCL) fibers aligned with 90° rotation in criss-cross patterns (see Figures 9 and 10). Material deposition is often linked to a particular brand of device, for example, 3D-Bioplotter System (EnvisionTEC, Gladbeck, Germany) was also used in work reported by Luo *et al.*<sup>61</sup> (see Figure 9). The authors demonstrated a method to create a 3D porous scaffold consisting of a network of hollow fibers (see Figure 9a–c). The fibers varied in diameter from 400/100 to 1, 190/450  $\mu\text{m}$  and were fabricated using the so-called “shell nozzle” that was constructed by inserting a smaller nozzle within the larger one. The material was a paste consisting of concentrated alginate (16%) and aqueous polyvinyl alcohol solution. The latter component, working as a viscosity modulator and a sacrificial porogen, was dissolved and subsequently washed with the  $\text{CaCl}_2$  solution during post-fabrication alginate cross-linking. To demonstrate system biocompatibility, the construct was seeded with human bone marrow mesenchymal stem cells. Viable cells were attached to both the inner and outer surfaces of hollow fibers. By combining the criss-cross plotting with a high concentration of extruded materials, it was possible to fabricate a porous construct with remarkable mechanical properties. Young’s modulus was up to 3 MPa for the wet construct and 50 MPa for a dry one. Nevertheless, cell encapsulation within the material was not discussed by the authors, probably due to the cytotoxic conditions of dispensing. Luo’s method of deposition of hollow fibers is particularly attractive for HVTE, as it can potentially yield a porous structure in which cell migration (and subsequent oriented ECM deposition) occurs along the length of the channels inside the threads.

The significant drawback when working with hydrogels is their poor mechanical strength. Therefore, improving and maintaining the mechanical integrity of the processed construct has become a key issue for 3D hydrogel structures. There is one possible way of addressing this matter as presented by Lee *et al.*<sup>62</sup> in his work on ear regeneration. In this case, 3D printing of PCL and cell-laden alginate was assisted by the deposition of polyethylene glycol (PEG) that served as a sacrificial layer to support the main structure. After complete fabrication, the PEG was removed, with no effect on cell viability. For “fabricating the ear”, adipocytes and chondrocytes encapsulated within the hydrogels were dispensed into the fat and cartilage regions, respectively (see Figure 9d, e). The role of PEG was to serve as a temporary support for constructs made out of PCL and cell-laden alginate. Building the HV requires forming the leaflets within the Valsalva; therefore, printing PEG, as a sacrificial support material for PCL, is an alternative way to perform free-form fabrication.

Kim *et al.*<sup>63</sup> and several other research groups investigated the use of hybrid materials consisting of stiff thermoplastic polymers and hydrogels. Their approach involves the combination of extruded micro-sized PCL (see Figure 10a, d, e), electrospun PCL nanofibers (see Figure 10b, f), and cell-laden alginate struts (see Figure 10c, g). Each layer consists of micro-sized PCL struts coated with PCL nanofibers that provide support to osteoblast-like cell-laden alginate. Such a hierarchical scaffold enables homogeneous mesenchymal stem cell attachment and proliferation (see Figure 10).<sup>64</sup>

Combining micro- and nanofibers of biopolymers supplemented with alginate hydrogels should trigger the attention of HVTE adepts for the following reasons. The HV scaffold must be geometrically stable and permanently fixed in the aortic root. For this purpose, the microfilaments constituting the

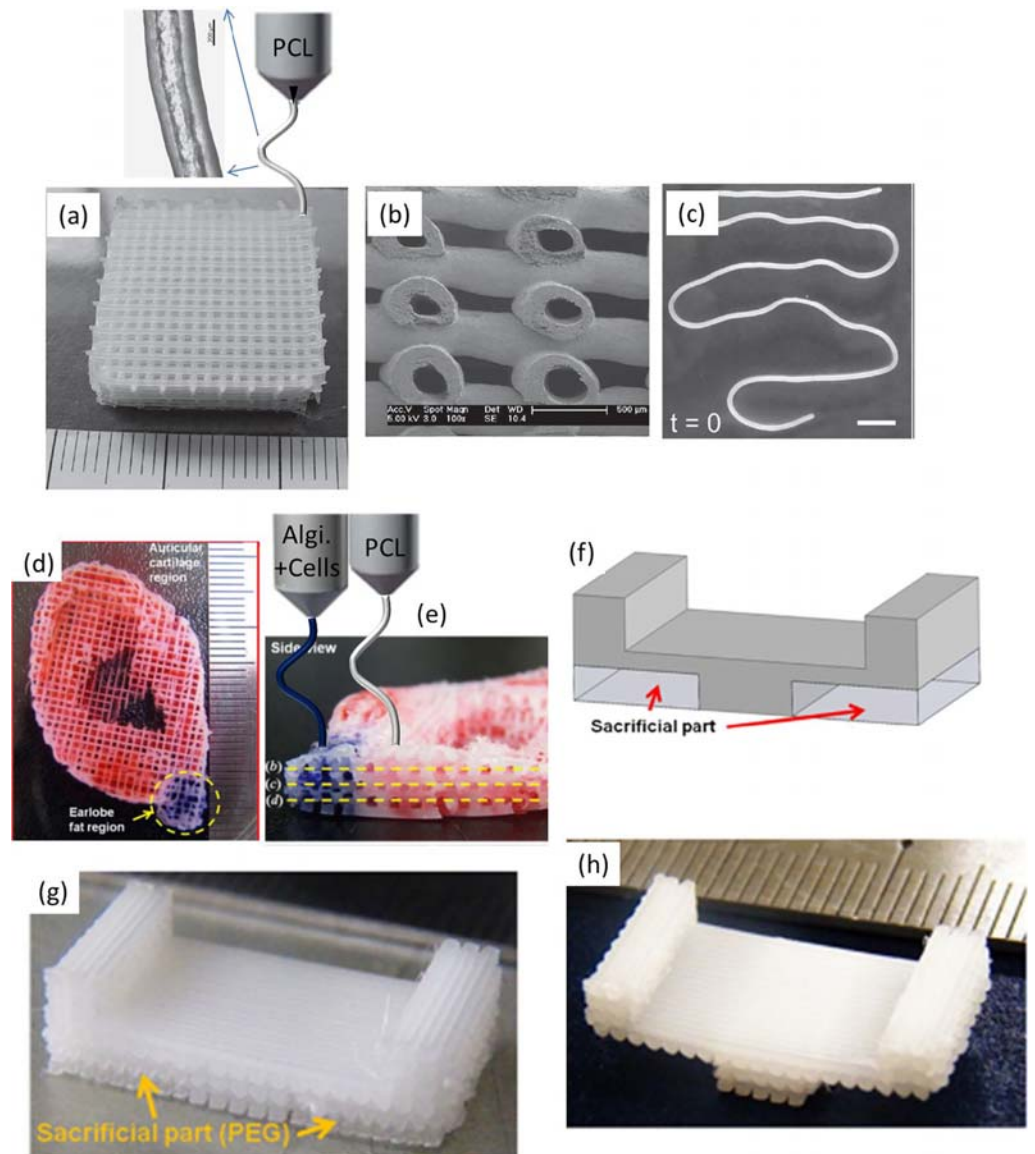


**Figure 9.** Hollow and PCL-enforced alginate scaffolds. (a) Macroscopic view of a 3D hollow fiber scaffold plotted with shell/core nozzles of 610/150  $\mu\text{m}$ . (b) SEM image of the hollow fiber scaffold plotted with shell/core nozzle. (c) Microscopic image of the plotted hollow fibers. Scale bar: 5 mm. Reprinted with permission from <sup>61</sup>. (d) Top and (e) side views of the printed cellular structure using 3D bioprinting technology with the sacrificial layer process. The lobe region is indicated in blue and auricular cartilage region is indicated in red. CAD designs of (f) the main part of PCL and sacrificial part of PEG, (g) PCL structure overhanging PEG support, and (h) PCL structure after removing the PEG with distilled water. Reprinted with permission from <sup>62</sup>.

stent-like structure should be superior. Certainly, those durable filaments will leak when they come in contact with blood. Therefore, the nanofibers of biopolymers can be used to seal the structure and simultaneously be an environment for oriented cellular growth. To ensure specific cell and scaffold interaction, the alginates with enhanced cell affinity may be used. To control the fate of the recruited cells, alginate can be supplemented with growth factors, such transforming growth factor- $\beta$ .<sup>65</sup> Interestingly, in isolation, alginate hydrogels, micro- or nanofilaments cannot play their role within the scaffold.

Within extrusion-based systems in 3D printing of alginate hydrogels, the main challenges are low mechanical strength and accuracy, slow processing, requirement of precise control of material properties, toxicity of cross-linking agents, uncontrolled fusion within the construct (collapsing of pores and channels), and lack of predefined ECM protein orientation. Future development will need to focus on optimizing new hydrogel formulations that will improve material printability as well as engineering

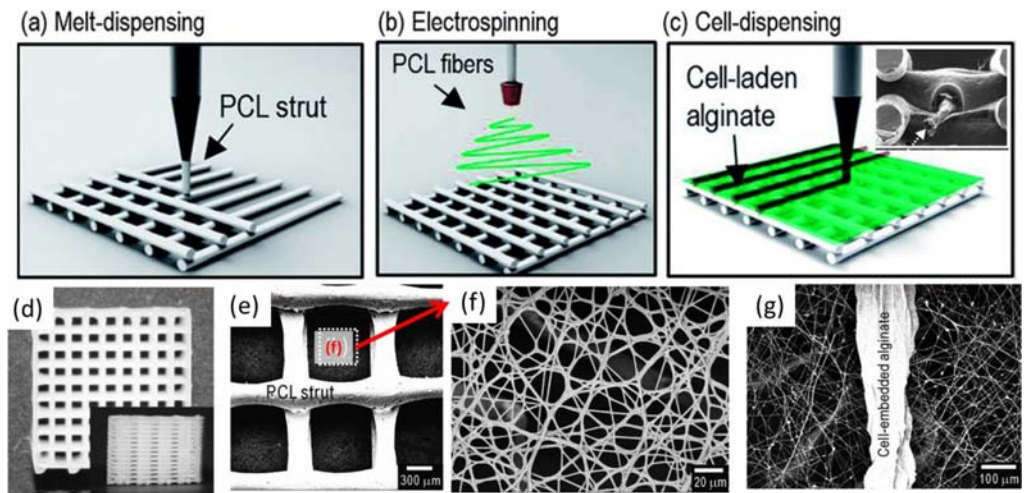


**Figure 10.** Cell-printed hierarchical scaffolds. (a–c) Schematic of scaffold fabrication. (d) Optical images of the PCL scaffold. (e) Micro-sized PCL. (f) Electrospun PCL nanofibers and (g) cell-laden alginate struts. Reprinted with permission from <sup>64</sup>.

new derivatives of alginate that would enable the precise control of mechanical parameters and structural anisotropy within the construct.

A promising solution, proposed by Hong *et al.*<sup>66</sup>, addressed some of the challenges highlighted above (see Figure 11). The authors created a PEG–alginate–nanoclay hydrogel that consisted of poly(ethylene glycol) diacrylate (PEGDA), sodium alginate, a photoinitiator, CaSO<sub>4</sub>, and encapsulated human embryonic kidney cells or human mesenchymal stem cells. The formulation was extruded to form a variety of shapes. Calcium ions cross-linked deposited alginate, which enabled the preservation of the shape of the hydrogel after printing. Printed objects were exposed to UV light to initiate the polymerization of PEGDA. The resulting construct was able to endure high stress in both tension and compression (see Figure 10b). Encapsulated cells showed viability at the level of 75% after one week of culture. They demonstrated a hydrogel that is 3D printable, strong, and suitable for cell culture.

### 7. 3D PRINTING OF ALGINATE HVTE

Expensive equipment is a substantial disadvantage when it comes to 3D printing of alginate. However, open-source, low-budget, extrusion-based systems have recently found their way into this research

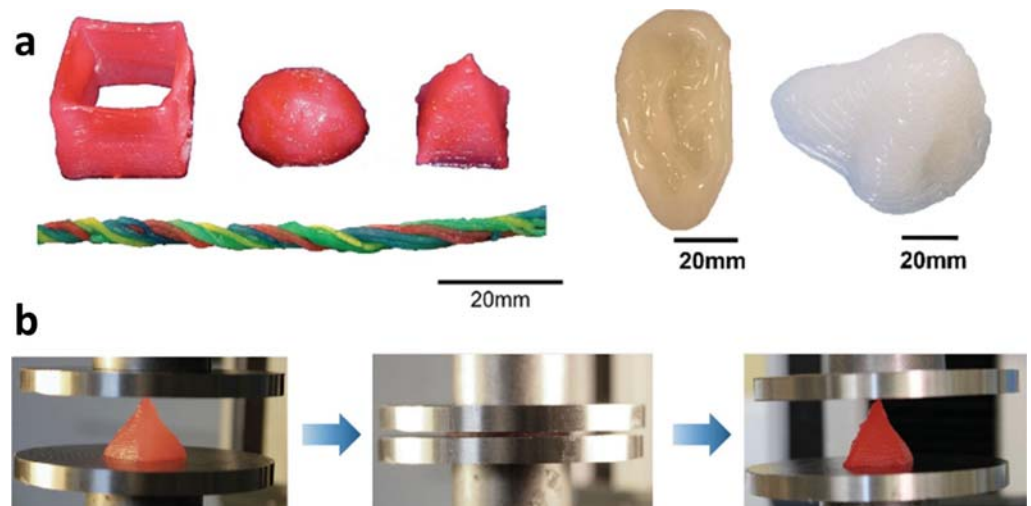


**Figure 11.** 3D printing of tough and biocompatible PEG–alginate–nanoclay hydrogels. (a) Various 3D constructs printed with the hydrogel. (b) A printed pyramid undergoes a compressive strain of 95% while returning to its original shape after relaxation. Reprinted with permission from <sup>66</sup>.

domain. A hydrogel-compatible example is the Fab@Home system.<sup>66</sup> This relatively cheap 3D printer (6,000 USD) has been used to construct aortic valves based on a (PEGDA)/alginate or alginate/gelatin blend.<sup>26,67</sup>

Duan *et al.*<sup>26</sup> used a Fab@Home biprinter to prepare scaffolds from gelatin/alginate-blended hydrogels. VICs and aortic root sinus smooth muscle cells (SMCs) were encapsulated separately into the alginate/gelatin blend before printing the HV root (using SMCs) and leaflets (using VICs). After one week of culture, the mechanical properties of the acellular scaffolds were found to be much lower than those of the cell-laden 3D printed hydrogels. This shows the importance of cell-dependent maturation of the construct (see Figure 12a). What is now needed is further advancement, focused on the role of the cells and cell-secreted proteins in enhancing the functionality of the construct.

The Fab@Home printer was also employed by Hockaday *et al.*<sup>67</sup> They demonstrated a photo cross-linking system with PEGDA hydrogel, used to 3D print heterogeneous and complex aortic valve scaffolds.<sup>67</sup> This excellently written manuscript could be referred to as an example of 3D fabrication based on the printing of the encapsulated cell, which is not the case.<sup>50</sup> To avoid confusion, the details of the cell embedding experiment are described below. In one variant of the experiment, aortic valve conduits were printed with the mixture of PEGDA/alginate. To temporarily increase viscosity during the printing extrusion process, an unmodified soluble alginate (15%, w/v) was mixed into PEGDA precursor formulations (PBS, photoinitiator, and PEGDA). The printed hydrogel was rinsed with phosphate-buffered saline overnight to leach out the non-cross-linked alginate. Following rotary cell seeding, the conduits were cultured in a flask. After three weeks of culture, it was found that due to the presence of alginate gel and the printed orientation, the engineered constructs from the blended hydrogel had a stiffness that was ten times greater than the scaffold constructs engineered from PEGDA only. It indicates that the prior scaffold system can withstand dynamic physiological pressures (see Figure 12b). One unanswered question is whether hydrogels containing PEGDA would be suitable for cell encapsulation, which increases the seeding efficiency of the fabricated structures.

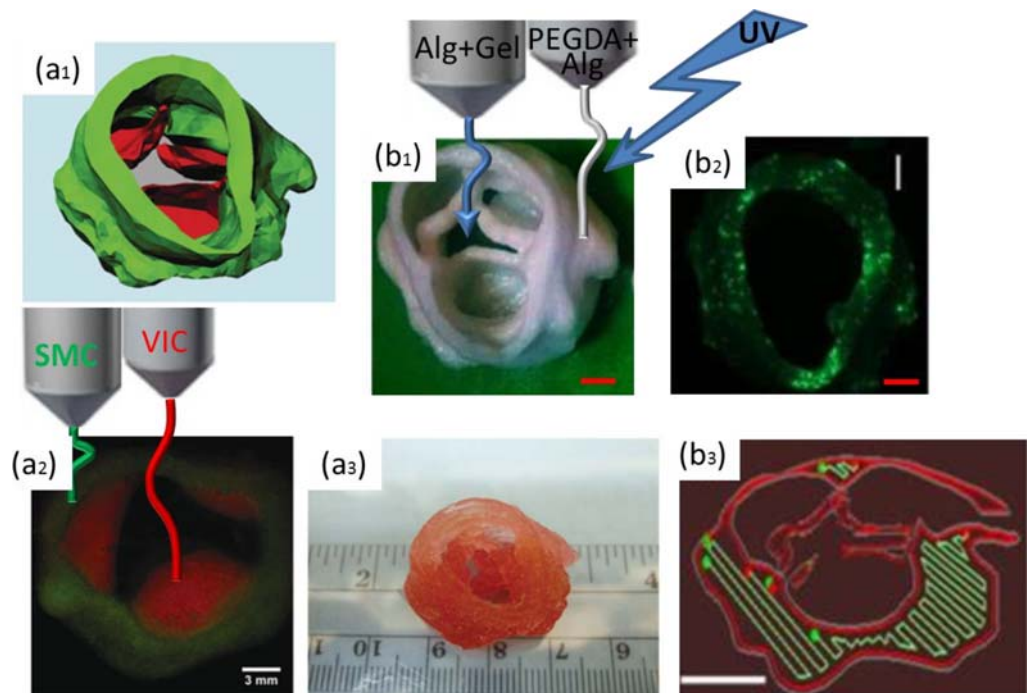


**Figure 12.** Bioprinting of the aortic valve conduit. Aortic valve model reconstructed from micro-CT images. (a<sub>1</sub>) The root and leaflet regions were rendered separately into 3D geometries into the stereolithography (STL) file format (red, valve leaflets; green, valve root). (a<sub>2</sub>) Fluorescent image of printed two layers of the aortic valve conduit. VIC for the valve leaflet was labeled by cell tracker indicated in red and SMC for the valve root were labeled by cell tracker indicated in green. (a<sub>3</sub>) As printed, alginate/gelatin aortic valve conduit. Reprinted with permission from <sup>26</sup>. (b<sub>1</sub>) Printed valve scaffold with 700 MW PEGDA/alginate. (b<sub>2</sub>) Live/dead imaging of PAVIC cultured on printed valve constructs. Live cells were visible both in the root and on the leaflets' surface for up to three weeks. Scale bars: 2 mm. (b<sub>3</sub>) Extrusion paths for each layer (red, contour; green, fill-in paths). Scale bars: 1 cm. Reprinted with permission from <sup>67</sup>.

## 8. ALTERNATIVE WAYS OF 3D CONSTRUCT FABRICATION USING ALGINATE FIBERS AND STRIPS

The extrusion method discussed above could be described as a process of assembling of freshly extruded threads. These threads are not usually interlaced, so there is a need to fuse them together (by melting or solving) to constitute the stable structure. Textile technologies may also be considered as a free-form fabrication method, in which the threads are produced in advance. The advantage of woven, knitted, and braided structures is interlacing of yarns that results in enhanced scaffold stability.<sup>68</sup> Examples of weaving alginate threads loaded with viable cells are highly relevant to HVTE and briefly summarized in Figure 13.<sup>10,11</sup> Here, cells are deposited directly into the dedicated location within the structure, avoiding time-consuming cellular diffusion through the construct (see Figure 13a, d).<sup>10,11</sup>

Organ weaving is a strategy based on assembling “living threads” consisting of alginate and encapsulated cells, enforced by polyester (PET) yarn.<sup>10</sup> “Living threads” are created by immersing threads that are soaked in a CaCl<sub>2</sub> solution into a sodium alginate-loaded cell suspension bath. Alginate encapsulation of the cells creates a bio-friendly, easily manageable starting material for building up the larger scaffold. Connecting different types of threads into 3D objects provides unique opportunities to construct the HV. However, new types of looms would be required to weave complex geometries of the HV (see Figure 13a–c).

Onoe *et al.*<sup>11</sup> created similar living threads using a microfluidic device with the double coaxial laminar flow. Meter-long core/shell alginate microfibers with encapsulated ECM proteins and differentiated cells or somatic stem cells were fabricated. The microfibers were assembled by weaving and reconstituted intrinsic morphologies and functions of living tissues. The generated fibers were very fragile; thus, limiting its use in free-form fabrication of the HV (see Figure 13d–f).

Careful preparation of threads before the assembling step has an additional advantage, as demonstrated by Leng *et al.*<sup>69</sup> Using the microfluidic device, they coded the continuous strip of the hydrogel. After winding on the roll, the bar constitutes the spatial object in which the location of cardiomyocytes was predefined (see Figure 13g–i). Combining this strategy with a high-throughput textile technique would virtually enable us to make large complex structures consisting of viable cells that may quickly mature, and has the potential to yield functional organs such as HVs.

## 9. 3D PRINTING-MEDIATED STRATEGY FOR DEVELOPING ALGINATE SPATIAL OBJECTS

The attractive alternative for providing alginates with desired shapes and components is to use highly precise 3D printing as an intermediate step of prototyping. To demonstrate this strategy, a scaffold reproducing the complex geometry of AHVs was obtained in a few easy steps. The geometrical and structural design of a typical AHV<sup>27,31,33,35</sup> was obtained using Blender<sup>70</sup> software (see Figure 2). The generated 3D file was converted into the STL format and 3D printed in Objet Eden260VS – 3D printer (Stratasys, Edina, Minnesota, USA) using light-curable polyacrylate monomers. After printing, the supporting material was manually removed, which yielded a flexible valve-like structure with sinuses of Valsalva and three coapting leaflets. Subsequently, agarose molds were obtained by casting agarose saturated in the solution of divalent cations into the 3D-printed form. Finally, the alginate scaffold was prepared by immersing agarose molds into alginate solutions. Calcium ions diffused from the agarose molds and efficiently cross-linked alginate solution in close vicinity, resulting in an alginate gel layer. The agarose molds could be easily removed in a subsequent step. The resulting alginate structure closely matched the agarose mold geometry and hence the 3D-printed replica of a human aortic valve (see Figure 14). Moreover, by extending the length of mold immersion into sodium alginate solutions, scaffold thickness and composition could be controlled. Such control would allow us to forecast further improvement in mechanical properties and to facilitate cellularization and tissue formation.

Alginate can form versatile and tunable hydrogels, which can be cast in 3D configurations that mimic the shape of a human aortic valve. As preparation steps can be freely adjusted to incorporate viable cells, such structures could serve as the basis for *in vitro* tissue formation, which would further improve mechanical properties of the hydrogel. Also, the ease of chemical modification and functionalization of alginate with cell ligands provides tools to increase cell interactions and attract cells *in situ*, which are necessary steps in the formation of functional valves *in vivo*.

Overall, this novel and flexible technique that can be readily integrated with other strategies presents a great potential to create the “ideal” scaffold for producing a living valve substitute.

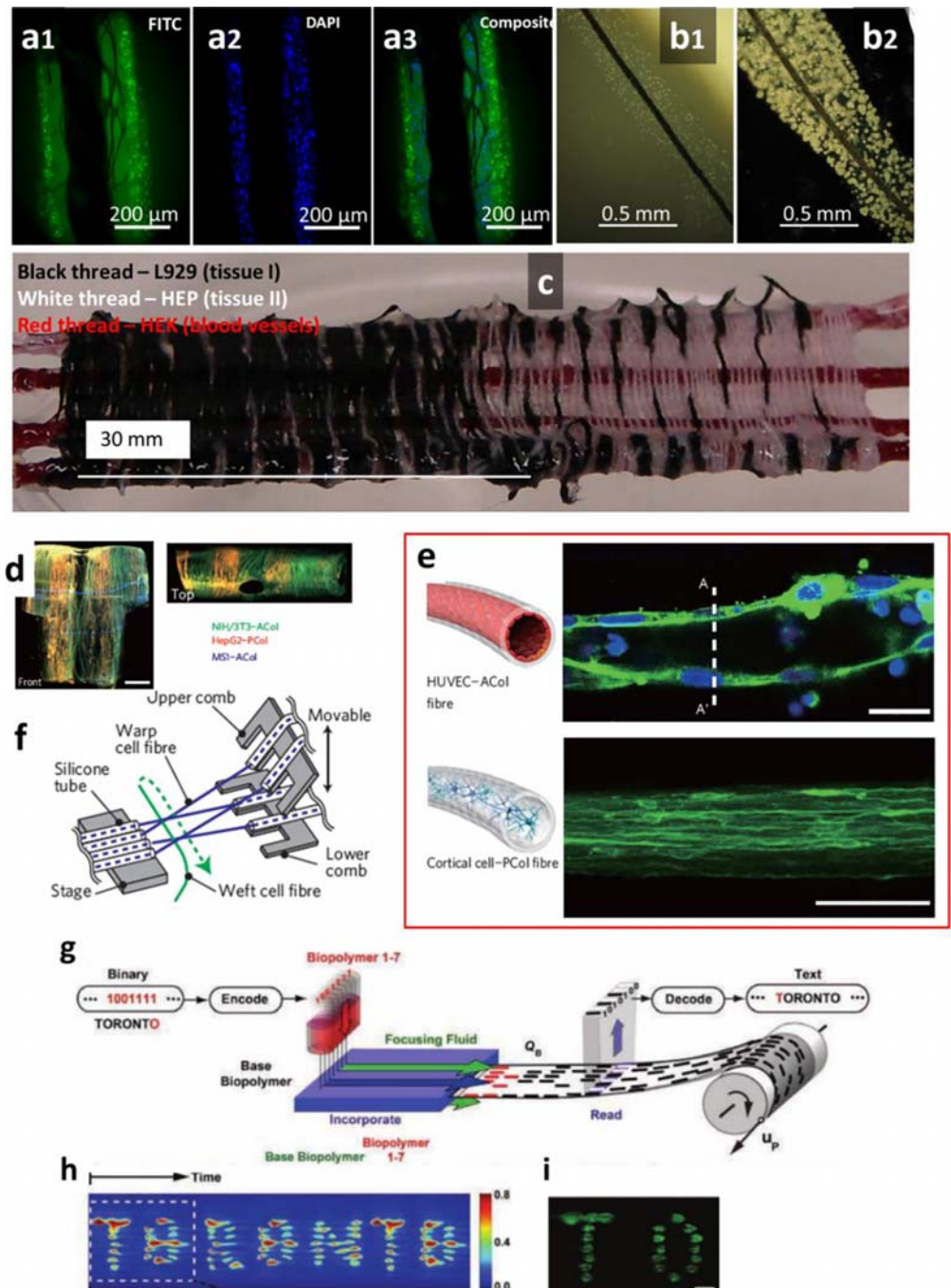


**Figure 13.** Alternative ways of 3D construct fabrication using alginate fibers and strips. Fiber-supported living threads, fluorescence images of the double-treated thread including fluorescently labeled L929 cells stained with (a1) CellTracker Green CMFDA and (a2) MCF-7 cells stained with nuclear stain Hoechst-33342. (a3) Overlay of images (a1) and (a2), showing two distinct layers of cells. (b1) Living thread immediately after preparation. (b2) The same after eight days of incubation. (c) Organ weaving: connecting tissues using gradients. An example of plain manual weaving using three cell lines. Reprinted with permission from <sup>10</sup>. (d) Fiber-based assembly of higher-order 3D macroscopic cellular structures. (e) Fluorescence micrograph of an HUVEC/ACol (top panel) and primary cortical cell/PCol fiber (bottom panel) at day 35. Scale bars: 20  $\mu$ m. (f) Schematic of a microfluidic weaving machine working in culture medium. Reprinted with permission from <sup>11</sup>. (g) Illustration of encoding information by dynamically incorporating spots of a secondary (fluorescently labeled) biopolymer into a base biopolymer and subsequently decoding the information contained in the hydrogel sheet. (h) Line camera intensity scan (top) and fluorescence image of encoded letters. (i) Fluorescence image of a pattern formed with 10 million/ml cardiomyocytes in 1.2% wt alginate and 0.08% wt collagen type I from a rat tail at day 0. Reprinted with permission from <sup>69</sup>.

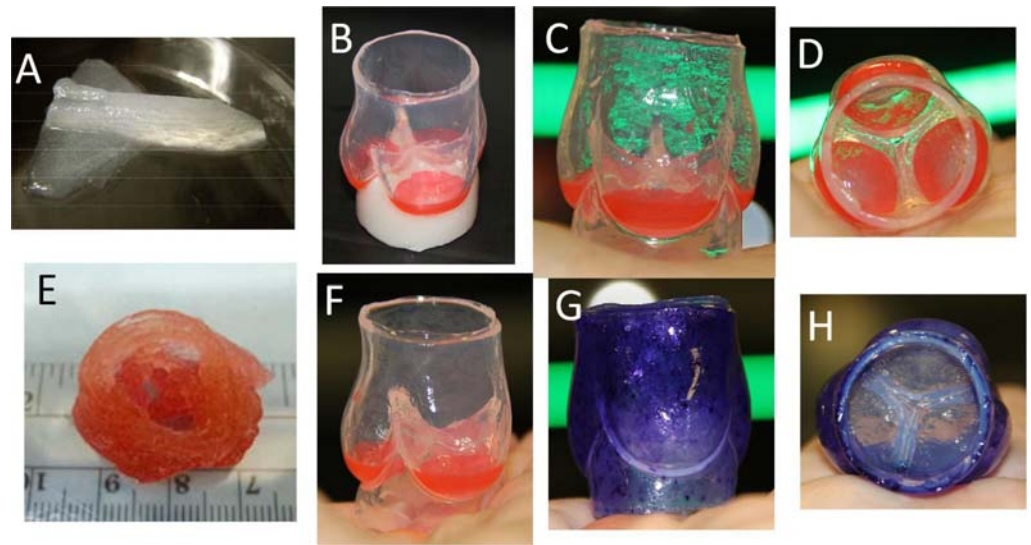


**Figure 14.** Alginate aircraft was printed with highest, previously reported resolution using the reactive extrusion method (A). Reprinted with permission from <sup>71</sup>. Alginate can form versatile, multicomponent, and tunable hydrogels. Multicomponent alginate valve on the (B) post and (C) after post-removal. (D) A view from the ventricular side. (E) HV printed with highest previously reported precision versus (F) HV obtained with 3D printing-assisted method. (G) Blue sinuses of Valsalva and transparent leaflets combined in one construct demonstrate the versatility of the method and endless options for governing alginate-based materials quickly and with high precision. Figure (E) was reprinted with permission from <sup>26</sup>.

#### 10. PERSPECTIVES OF 3D PRINTING OF ALGINATE FOR HVTE

The performance of the engineered valve ultimately depends on the self-assembling capacities of cells, the orientation of secreted proteins, and the cross-talk between the cells and the ECM. Therefore, the bioprinting of cellular microspheroids, which can work as bio-ink particles (as reported by Tan *et al.*<sup>72</sup>), is an attractive option for obtaining 3D structures such as HVs. In the first step, alginate solution was deposited on calcium-containing substrates in a layer-by-layer fashion to prepare 3D molds. Then, spheroids containing 50% endothelial cells and 50% SMCs were robotically placed into the 3D-printed alginate molds. The cells then fused into toroid-shaped tissue units. Immunofluorescence and histological analysis indicated that the cells secreted ECM proteins. This solution appears to be attractive from the perspective of calcium-free fabrication. However, only objects with simple geometry have been created so far (see Figure 15a). Further research in this field should focus on providing the inner mold areas with oriented biocompatible absorbable fibers together with peptides, enzymes, and growth factors that would control the direction of cellular growth and, as a result, the overall anisotropy of the system (see Figure 15b). The distinct disadvantage of the method, described by Tan *et al.*<sup>72</sup>, is that the complexity of the 3D mold structure is limited by the mechanical properties of the hydrogels and the removability of the mold after casting the cells.

To enable HVTE, mechanical robustness of the alginate could be further enhanced by combining alginate and acrylamide in formulations suitable for extrusion printing, as described by Bakarich *et al.*<sup>73</sup>. Ionic-covalent entanglement gels were fabricated through an extrusion printing process modified to facilitate in situ photopolymerization. The resulting hybrid gels exhibit an outstanding mechanical performance because the ionic cross-links in the biopolymer network act as sacrificial bonds that dissipate energy under stress.<sup>73</sup> The reversible nature of ionic cross-links of alginate could be exploited further, as shown in Figure 15b, and used as a temporary linker, which, after construct maturation, would enable sequential removal of the mold (see Figure 15b, left side).

Another possible way to obtain 3D-printed scaffolds with complex geometry and high cell viability is the photo cross-linking of cell-laden methacrylate-modified alginate.<sup>74</sup> The selection of photoinitiator is a matter of primary importance with regard to cell viability, which varies between 70 and 85% in this study after 48 h of culture. The long-term cytotoxicity of the unreacted acrylate moieties and the photoinitiator would need to be further investigated.

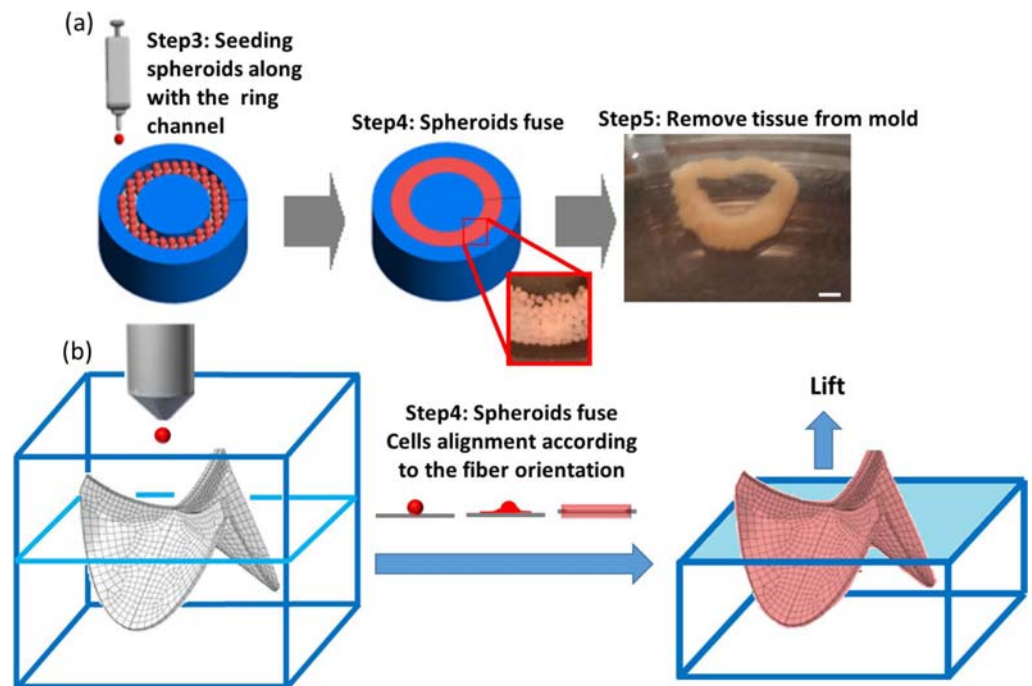


**Figure 15.** 3D alginate hydrogel printing for tissue unit fabrication. (a) Schematic (left side and center) and actual product (red square and right side) of casting the vascular spheroids containing endothelial cells and SMCs within the alginate mold. Scale bar: 1 mm. Reprinted with permission from <sup>72</sup>. (b) Hypothetical process of constructing a fiber-supported, spheroids-based construct for HVTE. Dark blue color represents covalently cross-linked hydrogel and light blue color represents reversibly cross-linked alginate that enables mold removal after cellular fusion and attachment to the fibers.

Another category of 3D deposition strategies that may play a pivotal role in alginate-based HVTE is the extrusion/aspiration patterning system. The aspiration process could be guided with higher precision than extrusion as cell viability is not a limiting factor. The 3D fabrication step consists of three modes, namely extrusion, aspiration, and refilling, which can potentially deliver excellent resolution, geometry, and complexity of the construct.<sup>75</sup> So far, however, there have not been any reports on applying that system to process an alginate hydrogel. Considering alginate's ability to be cross-linked reversibly, the potential of the method is noteworthy. From the perspective of HVTE, this approach can be used to pattern the cells on the surfaces of leaflets. By applying high suction, the groves on the leaflets may be provided. If groove width is sufficiently small, then cellular proliferation may be enhanced in an oriented manner, by geometrical restriction of cellular growth.

Another promising idea for alginate deposition is "suspended deposition 3D printing technology".<sup>76</sup> This system consists of two complementary hydrogels, one of which works as an omnidirectional gelatinous support medium, while the second may be 3D printed and suspended from the first (see Figure 16). Commercially available polyacrylate beads could serve as a suspension medium, while alginate can be deposited in the shapes that are not in the range of other processes (e.g., bridges). However, to date, there are only a few reports using this method for alginate deposition.<sup>77,78</sup>

Cui *et al.*<sup>79</sup> proposed light-triggered ionic cross-linking of alginates by incorporating a photosensitive  $\text{Ca}^{2+}$  cage. Upon irradiation, free  $\text{Ca}^{2+}$  was released from the cage, triggering local gelation of the alginate solution. By manipulating the radiation exposure dose, the authors were able to modulate mechanical properties of the hydrogel and the cross-linking degree and enhance homogeneity of the hydrogel compared with the mixture of alginate and soluble  $\text{Ca}^{2+}$  at comparable concentrations. For HVTE, the irradiation-dependent method of gelation provides an opportunity to govern the gelation with high precision and enables material patterning similar to photolithography techniques.

Bruchet *et al.*<sup>80</sup> reported a different approach with a similar effect. They prepared the alginate hydrogel cross-linked via  $\text{Fe}^{3+}$ . By exposure to 405 nm light in the presence of lactic acid,  $\text{Fe}^{3+}$  was reduced to  $\text{Fe}^{2+}$ , which cross-links the alginate less efficiently and makes the weaker gel easy to wash

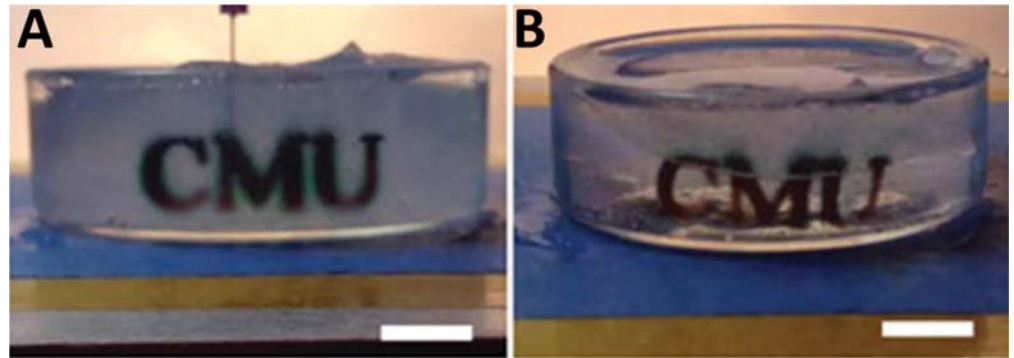


**Figure 16.** Freshly 3D-printed alginate in (A) suspension and (B) after  $\text{Ca}^{2+}$  release from the suspension medium. Scale bars: 1 cm. Reprinted with permission from <sup>77</sup>.

out. When the light was applied through the mask, then photolithography-like patterning of alginate was performed. Due to its biocompatibility, the approach appears potentially useful for advanced manipulation with cell culture, entrapping cells within the hydrogel or growing them on the surface. For HVTE, the advantage is that cells exposed to the light will be leached out of the construct, thus any mutagenic influence of light would not affect the leftover cells.

The prospective advances of alginate-based HVTE are not only determined by the progress in 3D deposition technologies, but also dependent on enhancing the properties of alginate as a biomaterial. The precise chemical degradation mechanism, timing, and approaches in the choice of alginate for drug delivery have been broadly reviewed.<sup>81</sup> More than 200 different alginate grades and alginate salts are now used. Multiple mechanisms can be considered to regulate the release speed of a compound using alginate. First, the size of the hydrogel can be controlled; a higher surface area will provide more “space” for the molecule to diffuse through the hydrogel. The density of the polymer, and thus the permeability of the hydrogel, can control the ease with which molecules can diffuse through the polymer network.

Several laboratories have demonstrated the use of alginate for the controlled delivery of angiogenic factors. The loss of ions in the alginate hydrogel can trigger its dissolution. Therefore, cross-linking could be used to improve the mechanical stability and control the degradation kinetics of the alginate hydrogel.<sup>82–84</sup> For example, vascular endothelial growth factor (VEGF) entrapped in the alginate hydrogel has a steady and continuous release for more than one month.<sup>85</sup> Free VEGF is degraded within 72 h post-injection, while VEGF injected into the alginate hydrogel is detectable up to 15 days after injection. Moreover, to enhance affinity to angiogenic factors, alginate can be sulfated, such that it mimics the structure of heparin.<sup>86</sup> This modification of the hydrogel has stronger binding to hepatocyte growth factor and achieves a higher therapeutic effect than the unmodified alginate. Collectively, this makes alginate an interesting candidate as a biomaterial for controlling the fate and performance of cells within the HV scaffold.

Hao *et al.*<sup>87</sup> investigated whether local sequential delivery of VEGF followed by platelet-derived growth factor-BB (PDGF-BB) with alginate hydrogels could induce a functional improvement and angiogenic effect that is greater than the single factors after myocardial infarction in a rat model]. Hydrogels were administered intramyocardially along the border of the myocardial infarction. Hydrogels comprised low- and high-molecular-weight alginate to enable the control of the release kinetics of incorporated factors.<sup>85</sup> Hydrogels were capable of delivering the growth factors sequentially. The VEGF was released faster than PDGF-BB. It led to a higher density of  $\alpha$ -smooth muscle actin positive vessels than in the case of single factors, but no increase was found in capillary density. Sequential protein delivery increased the systolic velocity-time integral and displayed a superior effect than single factors. In the aortic ring model, sequential delivery led to a higher angiogenic effect than single factor administration.<sup>87</sup> The authors concluded that applying the growth factors sequentially rather than individually could enhance the induction of mature vessels and the improvement of cardiac function. In the context of HVTE, rapidly degrading alginates embedded with growth factors may improve recruitment of cells on the scaffold, while slowly degrading alginates may provide drugs that may protect colonizing cells from calcification, for example.

## 11. CONCLUSIONS

A careful reader of our review may be startled by our hesitation in declaring 3D scaffold printing as advantageous, compared with other scaffold preparation methods<sup>88</sup> such as gas foaming,<sup>89</sup> phase separation,<sup>90</sup> electrospinning,<sup>91</sup> porogen leaching,<sup>92</sup> fiber mesh,<sup>93</sup> fiber bonding,<sup>94</sup> self-assembly,<sup>95</sup> membrane lamination,<sup>96</sup> and freeze drying.<sup>18</sup> According to our assessment, such a declaration would be misleading. The advantages of scaffold 3D printing include the ability to fabricate scaffolds with homogeneous cell distribution and complex architecture.<sup>97</sup> However, its drawback lies in scaffold production time.<sup>98,99</sup> Based on the results presented in Section 9, we conclude that 3D printing may lead to outstanding results, especially when combined with other scaffold preparation methods. Thus, it should be considered complementary rather than superior.

There are a number of take-home messages highlighted in this review. The number of reports on 3D printing of alginate for HVTE is limited, so the field is open for research efforts. Functional construct of the HV depends on its complex architecture, and the most rational approach to providing it is to use a combination of inkjet and extrusion 3D deposition with other scaffold fabrication methods. Inkjet printing is slow, but single-cell resolution can be obtained. Extrusion-based printing is quick, but the resolution of printing is limited. Alginate, as a primary material, is a good candidate for HVTE as no thrombosis occurred when injected into the human heart. Groundbreaking research can also be performed with low-cost 3D printing platforms. 3D printing is not superior but complementary to other scaffold fabrication methods. The challenge of enhancing the durability of the alginate hydrogel was approached by using alginate in combination with other materials. The 3D printing methods in suspension provide a possible structure with complex architecture; thus, this may be an exciting direction for further development. Textile techniques are technologically more mature than 3D printing methods and should be considered as vital free-form fabrication tools. Coding the yarn enables us to obtain a spatial object with predefined localization of its structural components including cells. The review on 3D printing should be considered as a landmark, not as a complete summary of technological advances.

In the author's opinion, the development of open-source 3D printers is the most prominent milestone of the last decade in the field of solid free-form fabrication. It is easy to underestimate the importance of benefits resulting from the inter-relationships between science and the public. However, it could potentially trigger significant technological advancements. A good analogy is the computer revolution that evolved from scientific laboratories<sup>100</sup> and gained substantial traction when a variety of "garage" hobby projects entered into the public domain under the name of a personal computer. This movement grew stronger to change the face of the world and became the backbone of some of the most daring scientific projects, such as mapping of the human genome or the Human Brain Project. We speculate that the same may occur for 3D printing technologies, as it appeals to the most common and fundamental needs of humans, namely our needs of creation and beauty. Developments arising from outside the academic world should be carefully examined for their potential to grow and become real scientific breakthroughs, particularly in the field of HVTE.

## Acknowledgements

The author would like to acknowledge Aleksandra Liberska and Najma Latif for their input in improving the manuscript. This study was funded by the Sidra Medical and Research Center, Doha, Qatar.

## REFERENCES

- [1] Bidarra SJ, Barrias CC, Granja PL. Injectable alginate hydrogels for cell delivery in tissue engineering. *Acta Biomater.* 2014;10:1646–1662.
- [2] Lee DW, Choi WS, Byun MW, Park HJ, Yu Y-M, Lee CM. Effect of gamma-irradiation on degradation of alginate. *J Agric Food Chem.* 2003;51:4819–4823.
- [3] Kong HJ, Smith MK, Mooney DJ. Designing alginate hydrogels to maintain viability of immobilized cells. *Biomaterials.* 2003;24:4023–4029.
- [4] Vauchel P, Kaas R, Arhaliass A, Baron R, Legrand J. A new process for extracting alginates from *Laminaria digitata*: Reactive extrusion. *Food Bioprocess Technol.* 2008;1:297–300.
- [5] Hay ID, Ur Rehman Z, Ghafoor A, Rehm BHA. Bacterial biosynthesis of alginates. *J Chem Technol Biotechnol.* 2010;85:752–759.
- [6] Lee KY, Rowley JA, Eiselt P, Moy EM, Bouhadir KH, Mooney DJ. Controlling mechanical and swelling properties of alginate hydrogels independently by cross-linker type and cross-linking density. *Macromolecules.* 2000;33:4291–4294.

- [7] Park H, Kang S-W, Kim B-S, Mooney DJ, Lee KY. Shear-reversibly crosslinked alginate hydrogels for tissue engineering. *Macromol Biosci*. 2009;9:895–901.
- [8] Rhim J-W. Physical and mechanical properties of water resistant sodium alginate films. *LWT – Food Sci Technol*. 2004;37:323–330.
- [9] Jianqi H, Hong H, Lieping S, Genghua G. Comparison of calcium alginate film with collagen membrane for guided bone regeneration in mandibular defects in rabbits. *J Oral Maxillofac Surg Off J Am Assoc Oral Maxillofac Surg*. 2002;60:1449–1454.
- [10] Liberski AR, Delaney JT Jr., Schäfer H, Perelaer J, Schubert US. Organ weaving: Woven threads and sheets as a step towards a new strategy for artificial organ development. *Macromol Biosci*. 2011;11:1491–1498.
- [11] Onoe H, Okitsu T, Itou A, Kato-Negishi M, Gojo R, Kiriya D, Sato K, Miura S, Iwanaga S, Kuribayashi-Shigetomi K, Matsunaga YT, Shimoyama Y, Takeuchi S. Metre-long cell-laden microfibrils exhibit tissue morphologies and functions. *Nat Mater*. 2013;12:584–590.
- [12] Yoon H, Ahn S, Kim G. Three-dimensional polycaprolactone hierarchical scaffolds supplemented with natural biomaterials to enhance mesenchymal stem cell proliferation. *Macromol Rapid Commun*. 2009;30:1632–1637.
- [13] Swain S, Behera A, Beg S, Patra CN, Dinda SC, Sruti J, Rao ME. Modified alginate beads for mucoadhesive drug delivery system: An updated review of patents. *Recent Pat Drug Deliv Formul*. 2012;6:259–277.
- [14] Jeon O, Alt DS, Ahmed SM, Alsberg E. The effect of oxidation on the degradation of photocrosslinkable alginate hydrogels. *Biomaterials*. 2012;33:3503–3514.
- [15] Lee KY, Mooney DJ. Alginate: Properties and biomedical applications. *Prog Polym Sci*. 2012;37:106–126.
- [16] Lee RJ, Hinson A, Helgerson S, Bauernschmitt R, Sabbah HN. Polymer-based restoration of left ventricular mechanics. *Cell Transplant*. 2013;22:529–533.
- [17] Frey N, Linke A, Süsselbeck T, Müller-Ehmsen J, Vermeersch P, Schoors D, Rosenberg M, Bea F, Tuvia S, Leor J. Intracoronary delivery of injectable bioabsorbable scaffold (IK-5001) to treat left ventricular remodeling after ST-elevation myocardial infarction: A first-in-man study. *Circ Cardiovasc Interv*. 2014;7:806–812.
- [18] Ruvinov E, Cohen S. Alginate biomaterial for the treatment of myocardial infarction: Progress, translational strategies, and clinical outlook: From ocean algae to patient bedside. *Adv Drug Deliv Rev*. 2016;96:54–76.
- [19] Cabrales P, Tsai AG, Intaglietta M. Alginate plasma expander maintains perfusion and plasma viscosity during extreme hemodilution. *Am J Physiol Heart Circ Physiol*. 2005;288:H1708–H1716.
- [20] Al-Shamkhani A, Duncan R. Radioiodination of alginate via covalently-bound tyrosinamide allows monitoring of its fate *in vivo*. *J Bioact Compat Polym*. 1995;10:4–13.
- [21] Leor J, Tuvia S, Guetta V, Manczur F, Castel D, Willenz U, Petneházy O, Landa N, Feinberg MS, Konen E, Goitein O, Tsur-Gang O, Shaul M, Klapper L, Cohen S. Intracoronary injection of *in situ* forming alginate hydrogel reverses left ventricular remodeling after myocardial infarction in swine. *J Am Coll Cardiol*. 2009;54:1014–1023.
- [22] Gao W, Lin T, Li T, Yu M, Hu X, Duan D. Sodium alginate/heparin composites on PVC surfaces inhibit the thrombosis and platelet adhesion: Applications in cardiac surgery. *Int J Clin Exp Med*. 2013;6:259–268.
- [23] Finosh GT, Jayabalan M. Regenerative therapy and tissue engineering for the treatment of end-stage cardiac failure: New developments and challenges. *Biomatter*. 2012;2:1–14.
- [24] Dar A, Shachar M, Leor J, Cohen S. Optimization of cardiac cell seeding and distribution in 3D porous alginate scaffolds. *Biotechnol Bioeng*. 2002;80:305–312.
- [25] Leor J, Aboulafia-Etzion S, Dar A, Shapiro L, Barbash IM, Battler A, Granot Y, Cohen S. Bioengineered cardiac grafts: A new approach to repair the infarcted myocardium? *Circulation*. 2000;102:III56–III61.
- [26] Duan B, Hockaday LA, Kang KH, Butcher JT. 3D bioprinting of heterogeneous aortic valve conduits with alginate/gelatin hydrogels. *J Biomed Mater Res A*. 2013;101:1255–1264.
- [27] Chester AH, El-Hamamsy I, Butcher JT, Latif N, Bertazzo S, Yacoub MH. The living aortic valve: From molecules to function. *Glob Cardiol Sci Pract*. 2014;2014:52–77.
- [28] Yacoub MH, Takkenberg JJM. Will heart valve tissue engineering change the world? *Nat Clin Pract Cardiovasc Med*. 2005;2:60–61.
- [29] Dohmen PM, Konertz W. Tissue-engineered heart valve scaffolds. *Ann Thorac Cardiovasc Surg Off J Assoc Thorac Cardiovasc Surg Asia*. 2009;15:362–367.
- [30] Dohmen PM. Tissue engineered aortic valve. *HSR Proc Intensive Care Cardiovasc Anesth*. 2012;4:89–93.
- [31] Yacoub MH, Kilner PJ, Birks EJ, Misfeld M. The aortic outflow and root: A tale of dynamism and crosstalk. *Ann Thorac Surg*. 1999;68:S37–S43.
- [32] Arjunon S, Rathan S, Jo H, Yoganathan AP. Aortic valve: Mechanical environment and mechanobiology. *Ann Biomed Eng*. 2013;41:1331–1346.
- [33] Hasan A, Ragaert K, Swieszkowski W, Selimović S, Paul A, Camci-Unal G, Mofrad MR, Khademhosseini A. Biomechanical properties of native and tissue engineered heart valve constructs. *J Biomech*. 2014;47:1949–1963.
- [34] Tara S, Rocco KA, Hibino N, Sugiura T, Kurobe H, Breuer CK, Shinoka T. Vessel bioengineering. *Circ J Off J Jpn Circ Soc*. 2014;78:12–19.
- [35] Yacoub MH. In search of living valve substitutes. *J Am Coll Cardiol*. 2015;66:889–891.
- [36] Kang KH, Hockaday LA, Butcher JT. Quantitative optimization of solid freeform deposition of aqueous hydrogels. *Biofabrication*. 2013;5:035001.
- [37] Cohen DL, Lo W, Tsavaris A, Peng D, Lipson H, Bonassar LJ. Increased mixing improves hydrogel homogeneity and quality of three-dimensional printed constructs. *Tissue Eng Part C Methods*. 2011;17:239–248.
- [38] Liberski AR, Zhang R, Bradley M. *In situ* nanoliter-scale polymer fabrication for flexible cell patterning. *J Assoc Lab Autom*. 2009;14:285–293.
- [39] Boland T, Tao X, Damon BJ, Manley B, Kesari P, Jalota S, Bhaduri S. Drop-on-demand printing of cells and materials for designer tissue constructs. *Mater Sci Eng C*. 2007;27:372–376.
- [40] Bader A, Schilling T, Teebken OE, Brandes G, Herden T, Steinhoff G, Haverich A. Tissue engineering of heart valves—human endothelial cell seeding of detergent acellularized porcine valves. *Eur J Cardio-Thorac Surg Off J Eur Assoc Cardio-Thorac Surg*. 1998;14:279–284.

- [41] Xu T, Baicu C, Aho M, Zile M, Boland T. Fabrication and characterization of bio-engineered cardiac pseudo tissues. *Biofabrication*. 2009;1:035001.
- [42] Lee CSD, Moyer HR, Gittens RAI, Williams JK, Boskey AL, Boyan BD, Schwartz Z. Regulating *in vivo* calcification of alginate microbeads. *Biomaterials*. 2010;31:4926–4934.
- [43] Place ES, Rojo L, Gentleman E, Sardinha JP, Stevens MM. Strontium- and zinc-alginate hydrogels for bone tissue engineering. *Tissue Eng Part A*. 2011;17:2713–2722.
- [44] Mørch YA, Donati I, Strand BL, Skjåk-Braek G. Effect of  $\text{Ca}^{2+}$ ,  $\text{Ba}^{2+}$ , and  $\text{Sr}^{2+}$  on alginate microbeads. *Biomacromolecules*. 2006;7:1471–1480.
- [45] Arai K, Iwanaga S, Toda H, Genci C, Nishiyama Y, Nakamura M. Three-dimensional inkjet biofabrication based on designed images. *Biofabrication*. 2011;3:034113.
- [46] Chapron J, Hosney H, Torii R, Sedky Y, Dunya M, Yacoub MH. Lessons from detailed 3D models of the cardiac chambers after the Mustard operation. *Glob Cardiol Sci Pract*. 2013;2013:49.
- [47] Nishiyama Y, Nakamura M, Henmi C, Yamaguchi K, Mochizuki S, Nakagawa H, Takiura K. Development of a three-dimensional bioprinter: Construction of cell supporting structures using hydrogel and state-of-the-art inkjet technology. *J Biomech Eng*. 2009;131:035001.
- [48] Liberski AR, Delaney JT, Schubert US. “One cell – one well”: A new approach to inkjet printing single cell microarrays. *ACS Comb Sci*. 2011;13:190–195.
- [49] Park SA, Lee SH, Kim W. Fabrication of hydrogel scaffolds using rapid prototyping for soft tissue engineering. *Macromol Res*. 2011;19:694–698.
- [50] Billiet T, Vandenhoute M, Schelfhout J, Van Vlierberghe S, Dubruel P. A review of trends and limitations in hydrogel-rapid prototyping for tissue engineering. *Biomaterials*. 2012;33:6020–6041.
- [51] Xu M, Wang X, Yan Y, Yao R, Ge Y. An cell-assembly derived physiological 3D model of the metabolic syndrome, based on adipose-derived stromal cells and a gelatin/alginate/fibrinogen matrix. *Biomaterials*. 2010;31:3868–3877.
- [52] Gaetani R, Doevendans PA, Metz CHG, Alblas J, Messina E, Giacomello A, Sluijter JP. Cardiac tissue engineering using tissue printing technology and human cardiac progenitor cells. *Biomaterials*. 2012;33:1782–1790.
- [53] Zhao Y, Yao R, Ouyang L, Ding H, Zhang T, Zhang K, Cheng S, Sun W. Three-dimensional printing of HeLa cells for cervical tumor model *in vitro*. *Biofabrication*. 2014;6:035001.
- [54] Colazzo F, Sarathchandra P, Smolenski RT, Chester AH, Tseng Y-T, Czernuszka JT, Yacoub MH, Taylor PM. Extracellular matrix production by adipose-derived stem cells: Implications for heart valve tissue engineering. *Biomaterials*. 2011;32:119–127.
- [55] Gimble JM, Katz AJ, Bunnell BA. Adipose-derived stem cells for regenerative medicine. *Circ Res*. 2007;100:1249–1260.
- [56] Sales VL, Mettler BA, Engelmayr GC, Aikawa E, Bischoff J, Martin DP, Exarhopoulos A, Moses MA, Schoen FJ, Sacks MS, Mayer JE Jr. Endothelial progenitor cells as a sole source for ex vivo seeding of tissue-engineered heart valves. *Tissue Eng Part A*. 2010;16:257–267.
- [57] Li S, Xiong Z, Wang X, Yan Y, Liu H, Zhang R. Direct fabrication of a hybrid cell/hydrogel construct by a double-nozzle assembling technology. *J Bioact Compat Polym*. 2009;24:249–265.
- [58] Huang Y, He K, Wang X. Rapid prototyping of a hybrid hierarchical polyurethane-cell/hydrogel construct for regenerative medicine. *Mater Sci Eng C*. 2013;33:3220–3229.
- [59] Duffy CRE, Zhang R, How S-E, Lilienkamp A, Tourmiaire G, Hu W, West CC, de Sousa P, Bradley M. A high-throughput polymer microarray approach for identifying defined substrates for mesenchymal stem cells. *Biomater Sci*. 2014;2:1683–1692.
- [60] Cohen DL, Malone E, Lipson H, Bonassar LJ. Direct freeform fabrication of seeded hydrogels in arbitrary geometries. *Tissue Eng*. 2006;12:1325–1335.
- [61] Luo Y, Lode A, Gelinsky M. Direct plotting of three-dimensional hollow fiber scaffolds based on concentrated alginate pastes for tissue engineering. *Adv Healthc Mater*. 2013;2:777–783.
- [62] Lee J-S, Hong JM, Jung JW, Shim J-H, Oh J-H, Cho D-W. 3D printing of composite tissue with complex shape applied to ear regeneration. *Biofabrication*. 2014;6:024103.
- [63] Schuurman W, Khristov V, Pot MW, van Weeren PR, Dhert WJA, Malda J. Bioprinting of hybrid tissue constructs with tailorable mechanical properties. *Biofabrication*. 2011;3:021001.
- [64] Yeo M, Kim G. Cell-printed hierarchical scaffolds consisting of micro-sized polycaprolactone (PCL) and electrospun PCL nanofibers/cell-laden alginate struts for tissue regeneration. *J Mater Chem B*. 2013;2:314–324.
- [65] Paranya G, Vineberg S, Dvorin E, Kaushal S, Roth SJ, Rabkin E, Schoen FJ, Bischoff J. Aortic valve endothelial cells undergo transforming growth factor- $\beta$ -mediated and non-transforming growth factor- $\beta$ -mediated transdifferentiation *in vitro*. *Am J Pathol*. 2001;159:1335–1343.
- [66] Hong S, Sycks D, Chan HF, Lin S, Lopez GP, Guilak F, Leong KW, Zhao X. 3D printing of highly stretchable and tough hydrogels into complex, cellularized structures. *Adv Mater Deerfield Beach Fla*. 2015;27:4035–4040.
- [67] Hockaday LA, Kang KH, Colangelo NW, Cheung PYC, Duan B, Malone E, Wu J, Girardi LN, Bonassar LJ, Lipson H, Chu CC, Butcher JT. Rapid 3D printing of anatomically accurate and mechanically heterogeneous aortic valve hydrogel scaffolds. *Biofabrication*. 2012;4:035005.
- [68] Tamayol A, Akbari M, Annabi N, Paul A, Khademhosseini A, Juncker D. Fiber-based tissue engineering: Progress, challenges, and opportunities. *Biotechnol Adv*. 2013;31:669–687.
- [69] Leng L, McAllister A, Zhang B, Radisic M, Günther A. Mosaic hydrogels: One-step formation of multiscale soft materials. *Adv Mater Deerfield Beach Fla*. 2012;24:3650–3658.
- [70] Introduction – Blender Reference Manual [Internet]. [[http://www.blender.org/manual/getting\\_started/about\\_blender/introduction.html](http://www.blender.org/manual/getting_started/about_blender/introduction.html)]. Accessed 23 November 2015.
- [71] ABSTRACT – SFFo8\_Cohen.pdf [Internet]. [[http://creativemachines.cornell.edu/papers/SFFo8\\_Cohen.pdf](http://creativemachines.cornell.edu/papers/SFFo8_Cohen.pdf)]. Accessed 7 February 2016.
- [72] Tan Y, Richards DJ, Trusk TC, Visconti RP, Yost MJ, Kindy MS, Drake CJ, Argraves WS, Markwald RR, Mei Y. 3D printing facilitated scaffold-free tissue unit fabrication. *Biofabrication*. 2014;6:024111.

- [73] Bakarich SE, Panhuis M in het, Beirne S, Wallace GG, Spinks GM. Extrusion printing of ionic-covalent entanglement hydrogels with high toughness. *J Mater Chem B*. 2013;1:4939–4946.
- [74] Rouillard AD, Berglund CM, Lee JY, Polacheck WJ, Tsui Y, Bonassar LJ, Kirby BJ. Methods for photocrosslinking alginate hydrogel scaffolds with high cell viability. *Tissue Eng Part C Methods*. 2011;17:173–179.
- [75] Iwami K, Noda T, Ishida K, Morishima K, Nakamura M, Umeda N. Bio rapid prototyping by extruding/aspirating/refilling thermoreversible hydrogel. *Biofabrication*. 2010;2:014108.
- [76] Vervae E. The Suspended Deposition Project by Brian Harm is a new 3D printing concept (VIDEO) [Internet]. 3D Printing Event. [<http://www.3dprintingevent.com/the-suspended-deposition-project-by-brian-harm-is-a-new-3d-printing-concept-video/>]. Accessed 1 September 2014.
- [77] Hinton TJ, Jallerat Q, Palchesko RN, Park JH, Grodzicki MS, Shue H-J, Ramadan MH, Hudson AR, Feinberg AW. Three-dimensional printing of complex biological structures by freeform reversible embedding of suspended hydrogels. *Sci Adv*. 2015;1:e1500758.
- [78] Bhattacharjee T, Zehnder SM, Rowe KG, Jain S, Nixon RM, Sawyer WG, Angelini TE. Writing in the granular gel medium. *Sci Adv*. 2015;1:e1500655.
- [79] Cui J, Wang M, Zheng Y, Rodríguez Muñiz GM, del Campo A. Light-triggered cross-linking of alginates with caged  $\text{Ca}^{2+}$ . *Biomacromolecules*. 2013;14:1251–1256.
- [80] Bruchet M, Mendelson NL, Melman A. Photochemical patterning of ionically cross-linked hydrogels. *Processes*. 2013;1:153–166.
- [81] Tønnesen HH, Karlsen J. Alginate in drug delivery systems. *Drug Dev Ind Pharm*. 2002;28:621–630.
- [82] Eral HB, López-Mejías V, O'Mahony M, Trout BL, Myerson AS, Doyle PS. Biocompatible alginate microgel particles as heteronucleants and encapsulating vehicles for hydrophilic and hydrophobic drugs. *Cryst Growth Des*. 2014;14:2073–2082.
- [83] Chan AW, Whitney RA, Neufeld RJ. Kinetic controlled synthesis of pH-responsive network alginate. *Biomacromolecules*. 2008;9:2536–2545.
- [84] Chu H, Wang Y. Therapeutic angiogenesis: Controlled delivery of angiogenic factors. *Ther Deliv*. 2012;3:693–714.
- [85] Silva EA, Mooney DJ. Spatiotemporal control of vascular endothelial growth factor delivery from injectable hydrogels enhances angiogenesis. *J Thromb Haemost*. 2007;5:590–598.
- [86] Ruvinov E, Leor J, Cohen S. The effects of controlled HGF delivery from an affinity-binding alginate biomaterial on angiogenesis and blood perfusion in a hindlimb ischemia model. *Biomaterials*. 2010;31:4573–4582.
- [87] Hao X, Silva EA, Månsson-Broberg A, Grinnemo K-H, Siddiqui AJ, Dellgren G, Wårdell E, Brodin LA, Mooney DJ, Sylvén C. Angiogenic effects of sequential release of VEGF-A165 and PDGF-BB with alginate hydrogels after myocardial infarction. *Cardiovasc Res*. 2007;75:178–185.
- [88] Subia B, Kundu J, Kundu SC. Biomaterial Scaffold Fabrication Techniques for Potential Tissue Engineering Applications. 2010 [<http://www.intechopen.com/books/tissue-engineering/biomaterial-scaffold-fabrication-techniques-for-potential-tissue-engineering-applications>]. Accessed 9 February 2016.
- [89] Harris LD, Kim BS, Mooney DJ. Open pore biodegradable matrices formed with gas foaming. *J Biomed Mater Res*. 1998;42:396–402.
- [90] Pavia FC, La Carrubba V, Piccarolo S, Brucato V. Polymeric scaffolds prepared via thermally induced phase separation: Tuning of structure and morphology. *J Biomed Mater Res A*. 2008;86:459–466.
- [91] Sohler J, Carubelli I, Sarathchandra P, Latif N, Chester AH, Yacoub MH. The potential of anisotropic matrices as substrate for heart valve engineering. *Biomaterials*. 2014;35:1833–1844.
- [92] Delaney JT, Liberski AR, Perelaer J, Schubert US. Reactive inkjet printing of calcium alginate hydrogel porogens—a new strategy to open-pore structured matrices with controlled geometry. *Soft Matter*. 2010;6:866–869.
- [93] Aibibu D, Hild M, Wöltje M, Cherif C. Textile cell-free scaffolds for *in situ* tissue engineering applications. *J Mater Sci Mater Med* [Internet]. 2016;27:63-1:63-20. [<http://www.ncbi.nlm.nih.gov/pmc/articles/PMC4723636/>]. Accessed 9 February 2016.
- [94] Mikos AG, Temenoff JS. Formation of highly porous biodegradable scaffolds for tissue engineering. *Electron J Biotechnol*. 2000;3:23–24.
- [95] Peck M, Dusserre N, McAllister TN, L'Heureux N. Tissue engineering by self-assembly. *Mater Today*. 2011;14:218–224.
- [96] Amensag S, McFetridge PS. Tuning scaffold mechanics by laminating native extracellular matrix membranes and effects on early cellular remodeling. *J Biomed Mater Res A*. 2014;102:1325–1333.
- [97] Do A-V, Khorsand B, Geary SM, Salem AK. 3D printing of scaffolds for tissue regeneration applications. *Adv Healthc Mater*. 2015;4:1742–1762.
- [98] Leong KF, Cheah CM, Chua CK. Solid freeform fabrication of three-dimensional scaffolds for engineering replacement tissues and organs. *Biomaterials*. 2003;24:2363–2378.
- [99] Hribar KC, Soman P, Warner J, Chung P, Chen S. Light-assisted direct-write of 3D functional biomaterials. *Lab Chip*. 2014;14:268–275.
- [100] Burks AW. The invention of the universal electronic computer—how the Electronic Computer Revolution began. *Future Gener Comput Syst*. 2002;18:871–892.